THE COMPANY OF **Biologists**

RESEARCH ARTICLE

Machine learning classification of cell-specific cardiac enhancers uncovers developmental subnetworks regulating progenitor cell division and cell fate specification

Shaad M. Ahmad[1],*, Brian W. Busser[1],*, Di Huang[2],*, Elizabeth J. Cozart[1], Sébastien Michaud[3], Xianmin Zhu[1], Neal Jeffries[4], Anton Aboukhalil[3,5], Martha L. Bulyk[3,6,7], Ivan Ovcharenko[2],‡ and Alan M. Michelson[1],‡

ABSTRACT

The *Drosophila* heart is composed of two distinct cell types, the contractile cardial cells (CCs) and the surrounding non-muscle pericardial cells (PCs), development of which is regulated by a network of conserved signaling molecules and transcription factors (TFs). Here, we used machine learning with array-based chromatin immunoprecipitation (ChIP) data and TF sequence motifs to computationally classify cell type-specific cardiac enhancers. Extensive testing of predicted enhancers at single-cell resolution revealed the added value of ChIP data for modeling cell type-specific activities. Furthermore, clustering the top-scoring classifier sequence features identified novel cardiac and cell type-specific regulatory motifs. For example, we found that the Myb motif learned by the classifier is crucial for CC activity, and the Myb TF acts in concert with two forkhead domain TFs and Polo kinase to regulate cardiac progenitor cell divisions. In addition, differential motif enrichment and *cis-trans* genetic studies revealed that the Notch signaling pathway TF Suppressor of Hairless [Su(H)] discriminates PC from CC enhancer activities. Collectively, these studies elucidate molecular pathways used in the regulatory decisions for proliferation and differentiation of cardiac progenitor cells, implicate Su(H) in regulating cell fate decisions of these progenitors, and document the utility of enhancer modeling in uncovering developmental regulatory subnetworks.

KEY WORDS: Machine learning, Gene regulation, Transcription factors, Progenitor specification, Cell division, Organogenesis, *Drosophila*

INTRODUCTION

A comparison of the molecular mechanisms governing heart development in *Drosophila* and vertebrates reveals a remarkable conservation of all major regulatory components, including both signals and transcription factors (TFs) (Olson, 2006; Bodmer and Frasch, 2010). Moreover, mutations in many of these conserved regulators of heart development have been shown to cause congenital heart disease in man (Bodmer and Frasch, 2010). Thus, understanding mechanisms of cardiogenesis in *Drosophila* can inform and guide similar analyses in vertebrate species, including human.

The formation of a complex organ such as the *Drosophila* heart involves the coordination of a diverse array of developmental processes, such as cell fate specification, differentiation and diversification (Bodmer and Frasch, 2010), by transcriptional regulation through enhancers (Davidson, 2006). Enhancers are stretches of DNA composed of DNA subsequences recognized by sequence-specific DNA-binding TFs that integrate the activity of tissue-specific, cell-specific, ubiquitously expressed and signal-activated TFs to guide gene expression programs at the level of both individual cells and the particular developmental steps that those cells undergo (Davidson, 2006; Busser et al., 2008). Recent genome-scale studies in *Drosophila* have confirmed the crucial role of transcriptional regulation in orchestrating cardiogenesis (Liu et al., 2009; Ahmad et al., 2012; Junion et al., 2012; Jin et al., 2013).

The *Drosophila* heart is a linear tube composed of two classes of cells: an inner row of contractile cardial cells (CCs) and an outer layer of non-muscle pericardial cells (PCs). Although CCs and PCs can be distinguished on the basis of morphological differences, unique lineages and the cell-specific expression patterns of distinct TFs (Bodmer and Frasch, 2010), little is known about the molecular mechanisms that underlie these cell-specific differences.

We previously used a machine learning approach to decipher the motifs and enhancers that govern the gene expression patterns of *Drosophila* muscle founder cells (Busser et al., 2012a), fusion competent myoblasts (Busser et al., 2012c) and cells of the human heart (Narlikar et al., 2010). Here, we utilized a similar multidimensional research strategy involving a combination of machine learning, array-based ChIP data for key mesodermal regulators, and experimental analyses to computationally classify, predict and validate cell type-specific cardiac enhancers and the crucial TF binding sites that are responsible for their activities. This integrative approach also enabled us to identify regulators of cell specification in the heart, and to characterize a molecular pathway involving two forkhead domain TFs, Myb and Polo kinase, which together mediate appropriate progenitor cell divisions in the heart. In addition, our findings allowed us to document a molecular mechanism for how Su(H) acts in the Notch signaling pathway to transcriptionally regulate the cell fates acquired by particular cardiac progenitors.

[1]Laboratory of Developmental Systems Biology, National Heart Lung and Blood Institute, National Institutes of Health, Bethesda, MD 20892, USA. [2]Computational Biology Branch, National Center for Biotechnology Information, National Library of Medicine, National Institutes of Health, Bethesda, MD 20892, USA. [3]Division of Genetics, Department of Medicine, Brigham and Women's Hospital and Harvard Medical School, Boston, MA 02115, USA. [4]Office of Biostatistics Research, National Heart Lung and Blood Institute, National Institutes of Health, Bethesda, MD 20892, USA. [5]Department of Aeronautics and Astronautics, Massachusetts Institute of Technology, Cambridge, MA 02139, USA. [6]Department of Pathology, Brigham and Women's Hospital and Harvard Medical School, Boston, MA 02115, USA. [7]Harvard-MIT Division of Health Sciences and Technology (HST), Harvard Medical School, Boston, MA 02115, USA.
*These authors contributed equally to this work

‡Authors for correspondence (ovcharen@nih.gov; michelsonam@nhlbi.nih.gov)

Development

RESULTS

Rationale and overview

Cardiogenesis involves multiple biological processes acting in concert during development. This coordination is achieved by the regulation of diverse cardiac genes by a finite set of cell-specific, tissue-specific, signal-activated and ubiquitously expressed TFs that drive heart gene expression. Thus, certain combinations of TF binding *in vivo*, as well as binding motifs for these TFs, constitute sequence features that are expected to be enriched in heart enhancers compared with other regions of DNA. The goal of this study was to take advantage of this distinct distribution of sequence features to build computational models that discriminate known cardiac enhancers from the rest of the genome, and to use this information in turn to predict novel cardiac enhancers, to identify the DNA sequence features (i.e. unique combinations of TF binding motifs) that act as positive predictors of cardiac cell type-specific enhancers, and to functionally validate the roles of these sequence features and their associated TFs in cardiogenic regulatory networks.

The strategy we used to achieve this objective is outlined in Fig. 1. First, we compiled training sets of known enhancers expressed in different cardiac cell subtypes. We next mapped known TF binding motifs from public databases and ChIP signals corresponding to *in vivo* TF binding to these training sets and control sequences. This

sequence annotation data along the DNA sequence of cardiac enhancers was then used by machine learning classification algorithms (classifiers) to separate cardiac enhancer sequences from controls. The reliability and efficacy of these cell type-specific classifiers were examined and compared by multiple approaches including a statistical analysis of enrichment of predicted enhancers in the loci of concordantly expressed genes followed by experimental validation of the functional specificity of enhancer predictions using transgenic reporter assays. Finally, the TF weights estimated by this computational classification were utilized to define and determine the role of novel TF binding motifs and their corresponding TFs in *cis* and *trans* assays based on the premise that a positive TF weight indicates a TF that is positively associated with heart activity.

Training sets of enhancers active in the *Drosophila* heart and individual cardiac cell subtypes

The PCs and CCs of the heart develop from a population of progenitor cells derived from the dorsal-most mesodermal cells termed the cardiac mesoderm (CM) (Bodmer and Frasch, 2010). In order to build classifiers, i.e. computational models that can discriminate cardiac cell type-specific enhancers from other DNA sequences, we first compiled training sets of enhancers with activity
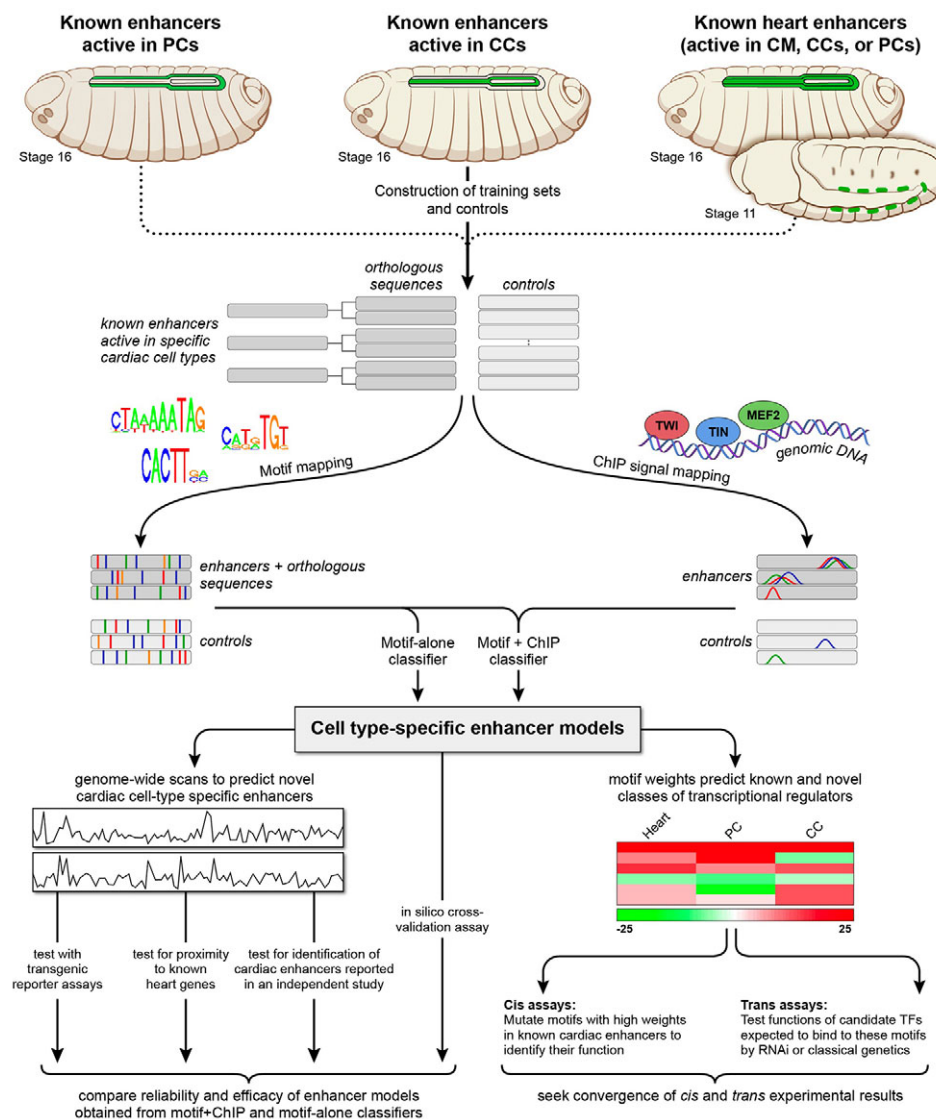

Fig. 1. Schematic overview of the computational and experimental strategy utilized in this study. Training sets of enhancers expressed in different cardiac cell types (increased in size through phylogenetic profiling) and control sequences were compiled and subsequently scanned to map sequence features corresponding to known binding site motifs collected from public databases and to *in vivo* TF binding signals obtained from published ChIP data profiles. Classifiers were built to create enhancer models that discriminate cell type-specific enhancers from respective controls. For each cell type, two classifiers were independently constructed: one based solely on motif features ('motif-alone') and the other on motif features and ChIP signals ('motif+ChIP'). The enhancer models were used to scan the *Drosophila* genome to identify novel cell-specific enhancers similar to the training sets, and the reliability and efficacy of the motif-alone and motif+ChIP classifiers for different cardiac cell types were examined and compared. Sequence features positively associated with computational classification were examined further using *cis* and *trans in vivo* experimental assays to identify and determine the functional roles of both the binding motifs and their associated regulatory TFs.

in the different cells of the *Drosophila* heart (Fig. 1). These included regions curated from the literature as well as a small set of unpublished enhancer sequences with activity in the heart (supplementary material Fig. S1), which we had previously identified and empirically verified (supplementary material Table S1). We sought to classify all cardiac enhancers by first compiling a training set of sequences with activity in any differentiated heart cells or their progenitors, including those unique to or active in any combination of PCs, CCs and CM (referred to hereafter as 'heart'; Fig. 1; supplementary material Table S1). We then attempted to refine this generic heart classification by categorizing expression in the individual subsets of the heart by training on sets of enhancers with activity in either PCs or CCs (supplementary material Table S1). Owing to the small size of the training sequences (23 heart enhancers, ten PC enhancers and 16 CC enhancers), and in order to avoid over-fitting decision rules learned by the classifier, we expanded these training sets using phylogenetic profiling (Busser et al., 2012a). Enhancer orthologs were extracted from the other 11 fully sequenced *Drosophila* species, mosquito, honeybee and red flour beetle by searching for regions with at least 50% but less than 80% sequence identity and similar length, GC content and repeat density as their *D. melanogaster* counterparts (supplementary material Table S1) (Busser et al., 2012a). Of note, we previously demonstrated the value of phylogenetic profiling as such orthologous sequences are active in the appropriate cells and their inclusion improves enhancer classification performance (Busser et al., 2012a). This approach led to a training set of 47 heart, 33 CC and 25 PC enhancer sequences (supplementary material Table S1).

Controls were generated by randomly sampling sequences from *D. melanogaster* non-coding regions with similar length, GC content and repeat content to the training enhancers (Fig. 1). Ten control sequences were retrieved for each training enhancer.

Accurate classification of cell-specific cardiac enhancers
Prior studies in *Drosophila* documented the difficulty in using machine learning for identifying cell- or tissue-specific enhancer activities simply by relying primarily on known TF binding motifs

from available databases (Kantorovitz et al., 2009; Busser et al., 2012a). We hypothesized that this poor performance might be improved with the inclusion of relevant ChIP data as an additional classifier feature (Busser et al., 2012a). Furlong and colleagues have previously determined the genome-wide binding profiles of a set of key *Drosophila* mesodermal regulatory TFs, including Tin, Twi and Mef2 (Zinzen et al., 2009). Because all three of these TFs are known to be required for cardiogenesis (Bodmer and Frasch, 2010), we included array-based ChIP data for these TFs as additional sequence features to build enhancer classifiers (Fig. 1). To investigate the contribution of their inclusion, we constructed separate classifiers for each training set that either added ChIP data ('motif+ChIP') or omitted this information ('motif-alone'). In this study, we used linear support vector machines (SVMs) as enhancer classifiers. SVMs are designed to identify combinations of sequence motifs that optimally separate enhancers from controls.

The ability of the classifiers to accurately predict regulatory activity was assessed by a tenfold cross-validation strategy (in which the original training set data was partitioned into complementary subsets, with one subset utilized to build the cell type-specific classifier, and the other subset used to validate the constructed classifier), with performance gauged by the area under the receiver operating characteristic curve (AUC). The AUC values for the motif-alone classifiers for heart, CC and PC enhancers are 0.85, 0.83 and 0.91, respectively, which suggests an accurate ability to discriminate appropriate enhancers from background sequences (Fig. 2A). The inclusion of ChIP data significantly improved the performance of each classifier, with AUC values increasing to 0.96 for heart enhancers, 0.96 for CCs and 0.97 for PCs (Fig. 2A). These results confirm that we are able to generate reliable classifiers, with significant improvements obtained with the inclusion of relevant ChIP data.

We next applied the developed classifiers to predict the presence of novel cardiac and cell type-specific enhancers throughout the *Drosophila* genome (supplementary material Table S2). These models predicted ~2000 enhancers at a false positive rate (FPR) of 0.01 for each cardiac cell type (supplementary material Fig. S2).
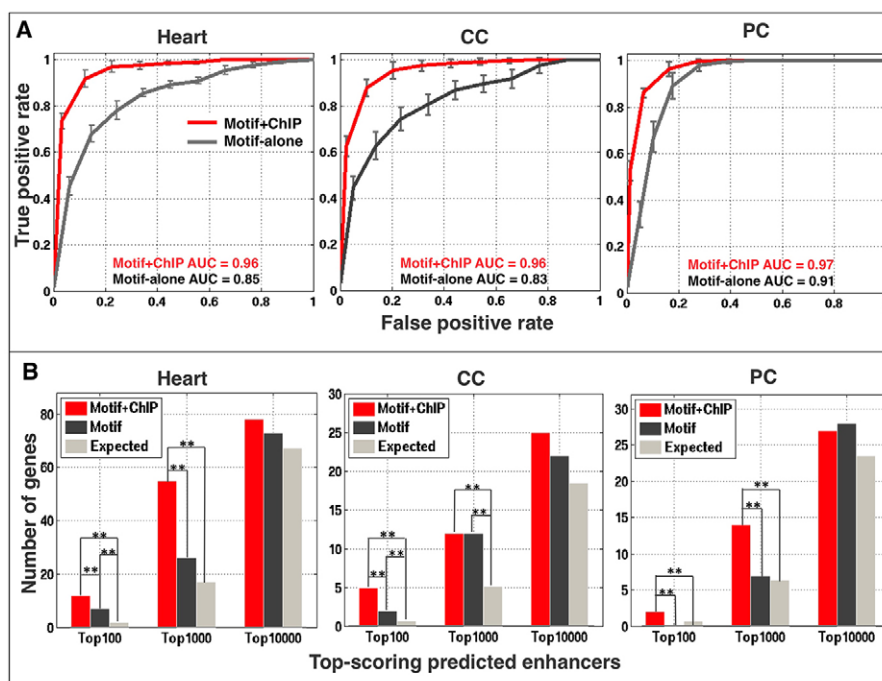

Fig. 2. Cell-specific cardiac enhancer classifiers perform with high specificity and sensitivity. (A) Average receiver operating characteristic curves and standard deviations for tenfold cross-validation performed for both motif-alone and motif+ChIP classifiers in 20 independent runs. (B) Enrichment in validated heart, CC and PC genes in the neighborhood of putative cardiac enhancers at different ranks for the motif-alone and motif+ChIP classifiers. Each of these genes is generally associated with only one prediction. Double asterisks indicate significant differences (*P*<0.005).

Putative enhancers are strongly associated with genes expressed in the corresponding cardiac cell type (Fig. 2B; supplementary material Tables S1, S2). Furthermore, the addition of the ChIP data significantly improved the enhancer model, as such predictions are more often associated with genes having known heart expression (Fig. 2B). Finally, all (100%) of the 28 cardiac enhancers reported in a recent study (Jin et al., 2013) that were not included in the training set were predicted by our motif+ChIP classifier for the heart at an FPR of 0.05, whereas 15 (53.6%) were identified by motif-alone (supplementary material Fig. S3; Table S2). Collectively, these results document the generation of classifiers that can reliably detect cell type-specific cardiac enhancers, and further show that the inclusion of ChIP data significantly improves the enhancer model.

Large-scale validation of cell-specific cardiac enhancers

To evaluate the *in vivo* functions of classifier-predicted enhancers, we used genomic site-specific transgenic reporter assays (Busser et al., 2012b; Busser et al., 2012a) to test 80 enhancer predictions with varying scores in the classifier rankings for the different enhancer models (supplementary material Table S2). Such analyses revealed that the top-scoring predictions for all classifications were often functional enhancers: 21 out of 41 (51.2%) top-scoring (i.e. <0.01 FPR) cardiac predictions were active in the heart, whereas 15 out of 37 (40.5%) top-scoring CC predictions were active in CCs, and 15 out of 31 (48.4%) top-scoring PC predictions were active in PCs (supplementary material Fig. S4A; Table S2). Not surprisingly, given that CCs and PCs define subsets of heart cells, many of these predictions were highly ranked in more than one classifier. For comparison, low scoring (>0.05 FPR) successful predictions were one out of 13 (7.7%), nine out of 38 (23.7%), and 11 out of 38 (28.9%) for heart, CC and PC classifiers, respectively.

These analyses also revealed that the classifiers that included ChIP data performed better in predicting functional enhancer activity on a genome-wide scale (supplementary material Fig. S4B). This result is most pronounced for the cell-specific classifiers, as many successful enhancer predictions for classifiers that relied solely on motifs were not included in the set identified with the relatively stringent 0.05 FPR cutoff. For example, whereas only 11 out of 20 successful motif-alone CC predictions (55.0%) and 13 out of 24 motif-alone successful PC predictions (54.1%) fell within the 0.05 FPR cutoff, 19 out of 20 successful CC predictions (95.0%) and 23 out of 24 successful PC predictions (95.8%) that utilized ChIP data also scored within this same cutoff (supplementary material Table S2; Fig. S4B). However, this difference was not seen for general heart predictions, as 25 out of 26 (96.2%) motif-alone and motif+ChIP predictions fell within the 0.05 FPR cutoff. These results suggest that the inclusion of ChIP data as an additional feature generates more reliable cell type-specific enhancer models, but is less necessary for predicting general cardiac activity.

Representative examples of transgenic embryos for top-scoring cardiac enhancer predictions are shown in Fig. 3, including those predicted regulatory elements associated with *senseless-2* (*sens-2*), *sprouty* (*sty*), *Trim9*, *CG9650* and *dally-like* (*dlp*) genes. Each of these predictions was highly ranked in both the heart and cell type-specific classifiers, and all were appropriately active in both CCs and PCs. Thus, both the cardiac and cell type-specific enhancer models are able to accurately predict appropriate *in vivo* reporter activity.

Interestingly, the predictions associated with the *rolling pebbles* (*rols*) and *Dorsocross 3* (*Doc3*) genes ranked much higher in the CC than in the PC classifier and indeed were found to be only active in CCs (Fig. 3). Conversely, the predictions associated with the *CG13822*, *Stromalin-2* (*SA-2*) and *CG14207* genes ranked much higher in the PC than in the CC classifier and were only active in PCs (Fig. 3). Thus, the distribution of enhancer ranks in these cell-specific classifications can be used to uncover cell-specific enhancer predictions.

Motif features associated with cardiac and cell type-specific enhancers

The analyses described above suggest that the sequence features learned by the classifier are sufficiently robust to predict cell type-specific cardiac enhancer activities. To understand these decision rules, we examined the sequence features positively associated with the classification of cardiac cell-type enhancers. For linear SVMs, features associated with the training set are given positive weights, those associated with the controls are given negative weights, and irrelevant features receive zero weight. The motifs most relevant to the heart and cell type-specific motif+ChIP classifications were then grouped according to the protein families of their respective TFs (Fig. 4). Similar results were seen with the motif-alone classification (supplementary material Fig. S5).

The presence of numerous known cardiac regulatory motifs, including those for NK-2 homeodomains (which include Tin), MADS box (which include Mef2) and basic helix-loop-helix (bHLH) TFs (which include Twi and Hand), as some of the most discriminating features of heart enhancers was an encouraging finding (Bodmer and Frasch, 2010). These motifs are likely to be directly occupied by the relevant regulatory TFs because the features representing Tin, Mef2 and Twi ChIP data are also highly weighted in the corresponding classifiers (supplementary material Table S3). Furthermore, additional enriched sequence features include previously characterized cardiac regulatory TFs, such as members of the GATA family, zinc finger family, LIM homeodomain family, Signal transducer and activator of transcription (Stat) and forkhead family of TFs (Bodmer and Frasch, 2010; Johnson et al., 2011; Ahmad et al., 2012; Zhu et al., 2012).

Interestingly, certain sequence features previously not known to play a role in heart development are enriched among all classifications. Such motifs include those recognized by the family of Myb domain TFs, which in *Drosophila* consists of a single ubiquitously expressed DNA-binding protein (Tomancak et al., 2007) that controls the regulation of proliferation or differentiation of progenitor cells (Ramsay, 2005), suggesting that Myb might be an unrecognized regulator of cardiogenesis. Finally, visualizing the separate classifications permits the identification of motifs that may discriminate PC and CC enhancer activities. For example, motifs for the Notch signaling pathway TF Su(H) are enriched in the PC classification and depleted in or irrelevant to the CC classification. This result suggests a role for Su(H) in governing the cell fate decision between PCs and CCs. In total, these results provide a comprehensive analysis of the motif preferences directing heart and cardiac cell type-specific gene expression programs.

Myb is an activator of the *Ndg* heart enhancer

Neither the CCs nor the PCs constitute a uniform population, as revealed both by their distinct cell lineages and by the complexity of their individual gene expression programs. From anterior to posterior, and named for the TFs they express, there are two Seven-up-CCs (Svp-CCs, unstained in Fig. 5A-C) and four Tinman-CCs (Tin-CCs, red in Fig. 5A-C) in each repeating hemisegment. In order to assess whether the Myb motif is functionally relevant to driving the activity of heart enhancers, we examined its potential role in the *Nidogen* (*Ndg*) cardiac enhancer (Philippakis et al., 2006). We
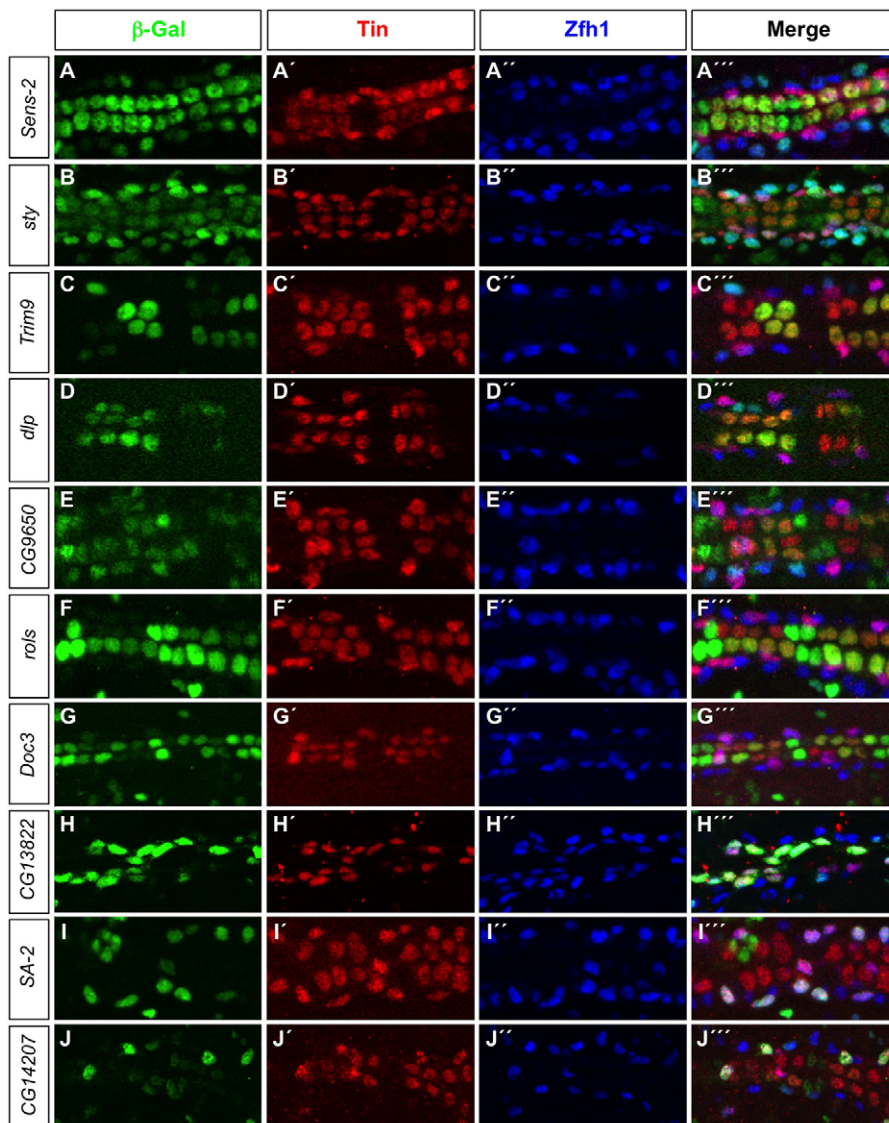
Fig. 3. Candidate enhancers predicted by the cell-specific cardiac classifiers are active in the appropriate cardiac cell types. (A-J‴) *lacZ* reporter gene activity (β-galactosidase, green) driven by classifier-predicted enhancers. All PCs are marked by Zfh1 expression (blue) whereas the posterior-most four CCs in each hemisegment, the Tin-PCs and the Eve-PCs are marked by Tin expression (red).

previously showed that the wild-type *Ndg* enhancer is active in only the two anteriormost Tin-CCs in a hemisegment (Fig. 5A,D; supplementary material Table S4) (Zhu et al., 2012) and contains three Myb motifs required for restricting somatic mesodermal enhancer activity (Busser et al., 2012a). Here we show that mutagenesis of these same Myb binding sites results in significant partial inactivation of the enhancer (*Ndg^{Myb}*) in CCs (Fig. 5B,D; supplementary material Table S4), thereby demonstrating the functional importance of these sites to cardiac activity.

We next determined whether a similar phenotype could be achieved by eliminating Myb function in *trans*. Embryos hemizygous for *Myb^{MH30}* (Manak et al., 2002), a chromosomal deficiency that completely deletes the *Myb* gene, do indeed exhibit significant partial inactivation of the wild-type enhancer (*Ndg^{WT}*) reporter (Fig. 5C,D; supplementary material Table S4).

The convergence of results for these *cis* and *trans* experiments suggests that Myb protein functionally activates the cardiac enhancer of at least one heart gene, thus providing a plausible rationale for the identification of Myb motifs as positive discriminators in the classification of CC, PC and heart enhancers. In turn, this finding raises the question of in which cardiogenic processes this TF might be involved.

Myb is required for two distinct categories of cardiac progenitor cell divisions

We undertook a more detailed analysis of the cardiogenic roles of Myb by examining embryos in which *Myb* activity was knocked down by CM and heart-targeted RNA interference (RNAi) directed by the *TinD-GAL4* (Yin et al., 1997) and *Hand-GAL4* (Han and Olson, 2005) drivers. Staining with appropriate antibodies showed hemisegments with localized increases and decreases in both Svp-CC and Tin-CC numbers, compared with control embryos (supplementary material Fig. S6). Similar cardiac phenotypes were also observed in embryos hemizygous for the *Myb^{MH30}* deficiency (Fig. 6A-D).

The localized changes in CC number in embryos lacking *Myb* function are reminiscent of the effects of cardiac progenitor cell division defects observed in embryos mutant for either of the two forkhead TF-encoding genes *jumu* or *CHES-1-like*, or for the downstream kinase-encoding gene *polo* (Ahmad et al., 2012). The two Svp-CCs in wild-type cardiac hemisegments are generated by two asymmetric progenitor cell divisions, with each division from an Svp progenitor cell producing one Svp-CC and one Svp-PC (Fig. 6E, yellow and red cells, respectively), whereas two symmetric cell divisions give rise to the four Tin-CCs (Fig. 6E, green cells)
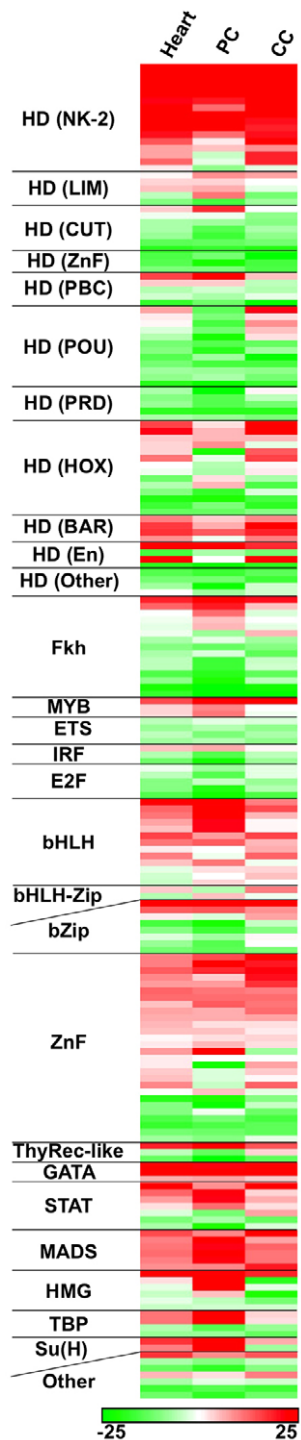
Fig. 4. Machine learning modeling of cardiac enhancers reveals sequence motif features that are relevant to their cell type-specific functional classification. A linear SVM was trained for each of three cardiac training sets (heart, PC and CC) using motif features and relevant ChIP data. TF binding motifs are ranked according to their linear SVM weights, with positive weights reflecting enrichment and negative weights reflecting depletion from the training set compared with background. TF binding motifs were grouped according to DNA-binding domain class of their respective TFs.

(Gajewski et al., 2000; Ward and Skeath, 2000; Han and Olson, 2005; Bodmer and Frasch, 2010). Eliminating *jumu*, *CHES-1-like* or *polo* function results in characteristic asymmetric and symmetric cell

division defects affecting the number of Svp heart cell types and Tin-CCs, respectively (Fig. 6E) (Ahmad et al., 2012). All three genes have also been implicated in cell divisions at an earlier developmental stage that generate the Svp progenitor cells, with mutations in these genes producing either one or three Svp progenitors per hemisegment in place of the expected two, thus subsequently resulting in one or three pairs of Svp-CCs and Svp-PCs, respectively (Ahmad et al., 2012). Note that each of these distinct types of cell division defects (schematically summarized in Fig. 6E) can be uniquely identified by assessing the number of Svp-CCs, Svp-PCs and Tin-CCs in a hemisegment by staining with appropriate markers.

We attempted to ascertain whether one or more of these cell division defects were also responsible for the localized changes in CC number detected in *Myb* mutants. Examination of embryos hemizygous for Myb^{MH30} revealed a significant increase over wild type both in the fraction of hemisegments with either excess or fewer Tin-CCs, corresponding to symmetric cell division defects, and in the fraction of hemisegments with either one or three pairs of Svp-CCs and Svp-PCs, corresponding to earlier cell division defects affecting the number of Svp progenitors (Fig. 6A-D,F; supplementary material Table S4). An alternative explanation for the latter phenotype is defective *Myb*-mediated selection of Svp progenitors from cardiac mesoderm equivalence groups. However, given the well-characterized role of *Myb* in governing mitosis and cytokinesis (Katzen et al., 1998; DeBruhl et al., 2013), we consider defects in earlier rounds of cell division to be the more likely cause. By contrast, the fraction of hemisegments exhibiting asymmetric cell division defects in Myb^{MH30} hemizygotes was both minuscule and not significantly different from that in wild-type embryos (Fig. 6F).

Collectively, these results indicate that *Myb* regulates two distinct categories of cardiac progenitor cell divisions to specify correct cardiac cell numbers: symmetric cell divisions of the Tin-CC progenitors, and an earlier round of cell divisions that gives rise to the Svp progenitors. The observations that these two classes of cell division are also mediated by a pathway involving *jumu* and *CHES-1-like* regulating *polo* (Ahmad et al., 2012), and that *Myb* itself also regulates *polo* in other systems (Wen et al., 2008), suggested that *Myb* too might be acting through the same pathway, a hypothesis that we examined in the following experiments.

Synergistic genetic interactions between *jumu*, *CHES-1-like*, *polo* and *Myb*

If *Myb* functions through the same pathway as *jumu*, *CHES-1-like* and *polo*, then strong pairwise genetic interactions are likely to occur between *Myb* and each of these genes. In order to assess this possibility, the cardiac phenotypes of single heterozygotes for mutations in these four genes were quantified and compared with those of embryos that were doubly heterozygous for mutations in both *Myb* and *jumu*, for mutations in both *Myb* and *CHES-1-like*, or for mutations in both *Myb* and *polo* (supplementary material Figs S7, S8; Table S4). Double heterozygotes for both *Myb* and *jumu* mutations exhibit symmetric cell division defects and earlier Svp cell division defects that are significantly more severe than the additive effects of each of the two single heterozygotes. Similar synergistic genetic interactions occur between *Myb* and *CHES-1-like* for both symmetric cell divisions and earlier cell divisions generating Svp progenitors, as well as between *Myb* and *polo*. Collectively, these results suggest that *Myb*, *jumu*, *CHES-1-like* and *polo* act through the same pathway to mediate these two classes of cardiac progenitor cell divisions.
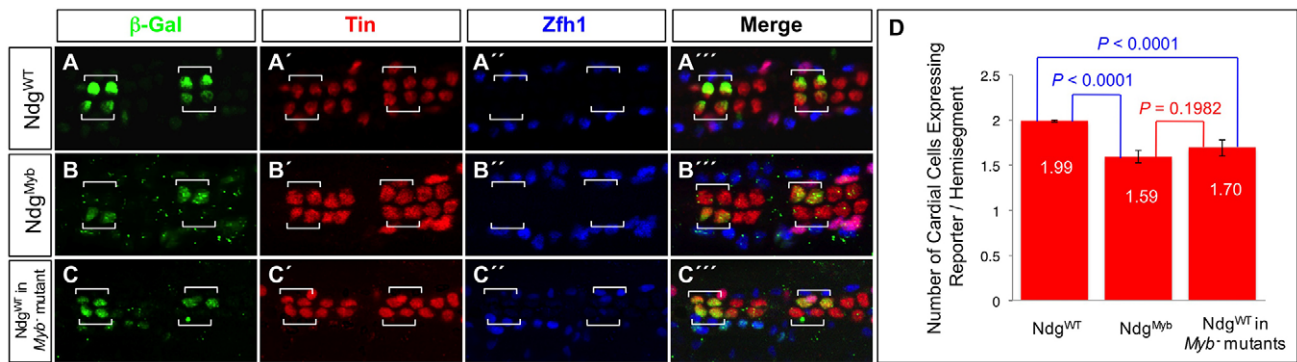
Fig. 5. Myb is an activator of the *Ndg* enhancer in the heart. (A-C‴) The posterior-most four CCs are marked by Tin expression (red), and the PCs are marked by Zfh1 expression (blue). (A-A‴) A β-galactosidase reporter (green) driven by the wild-type *Ndg* enhancer is expressed in only two Tin-expressing CCs per hemisegment (square brackets). (B-B‴) Mutations in the Myb binding sites result in partial but significant inactivation of reporter expression in these two CCs. (C-C‴) Reporter expression from the wild-type *Ndg* enhancer is also partially but significantly inactivated in these two CCs in embryos hemizygous for the *Myb^MH30* null mutation. (D) Histogram showing the mean number of CCs with 95% confidence intervals expressing the reporter and the significance of partial inactivation as a result of either the Myb binding site mutations in the *Ndg* enhancer or the *Myb^MH30* null mutation.

The Notch signaling pathway TF Su(H) discriminates between PC and CC enhancer activities

The observation that Su(H) motifs were positively weighted among PC sequences and were either depleted or irrelevant for the classification of CC sequences (Fig. 4; supplementary material Fig. S5) raised the possibility that Su(H) may act as a discriminator of these two cell types, which is supported by the expression of Su(H) in the CM (Tomancak et al., 2007). Furthermore, Su(H) is the terminal TF in the Notch signaling pathway, and inactivating mutations in other genes in the pathway, such as *Notch*, *Delta* or *sanpodo*, result in PC to CC transformations (Park et al., 1998; Gajewski et al., 2000; Ward and Skeath, 2000; Mandal et al., 2004; Grigorian et al., 2011), providing additional support for this hypothesis.

To test this model experimentally, we used site-directed mutagenesis to abolish the ability of Su(H) to recognize its well-characterized binding site (Rebeiz et al., 2011) in the PC enhancer of *Holes in muscle* (*Him*), a gene previously shown to be a direct target of Su(H) *in vivo* (Krejčí et al., 2009; Bernard et al., 2010), and assessed the effects of this mutation on enhancer function. The wild-type version of this enhancer (*Him^WT*) is active exclusively in all PCs of the differentiated heart (Fig. 7A), whereas mutagenesis of the Su(H) binding site in the *Him* enhancer [*Him^Su(H)*] induced additional ectopic reporter activity in all of the CCs without altering expression in PCs (Fig. 7B; supplementary material Fig. S9). Thus, Su(H) binding is necessary for repressing the activity of the *Him* enhancer in CCs, consistent with its well-characterized role in mediating transcriptional repression in other contexts (Bray and Furriols, 2001; Bray and Bernard, 2010).

In order to examine further the mechanism by which Su(H) normally represses the *Him* enhancer in CCs, and to avoid the pleiotropic effects of the Notch signaling pathway on additional tissues, we targeted gain and loss of function of Su(H) to cardiac progenitors. We reasoned that loss of Su(H) function by RNAi directed to the CM should lead to ectopic *Him* reporter activity in CCs, mimicking the loss of Su(H) binding sites in the *Him* enhancer. We confirmed this prediction by showing that the wild-type *Him* enhancer is indeed ectopically active in a subset of CCs in embryos in which Su(H) levels are depleted by RNAi knockdown (Fig. 7C). The fact that not all CCs express ectopic reporter activity probably reflects an incomplete RNAi knockdown of Su(H) levels in all progenitor cells.

In addition, we reasoned that the overexpression of the processed intracellular domain of Notch (N^icd), which has been shown to convert the Su(H) complex from a repressor into an activator for target genes (Bray and Furriols, 2001; Bray and Bernard, 2010), should induce ectopic activity of the *Him* gene in CCs. In agreement with this prediction, overexpression of N^icd in all cardiac progenitors by the *Hand-Gal4* driver (Han and Olson, 2005) induced ectopic expression of *Him*, which is normally restricted to PCs, in Mef2-expressing CCs (Fig. 7D,E). The disorganized heart cells and the very weak expression of Mef2 in CCs suggest that CC cell fate specification is highly abnormal in *Hand>N^icd* embryos, with the CCs in the process of being partly transformed to PCs. Nevertheless, this partial transformation of CCs to PCs also entails the ectopic expression of PC markers, and it is this latter process that is illustrated by the detection of *Him* transcript in CCs as a consequence of the overexpression of N^icd (Fig. 7E). Collectively, these results suggest that the Notch signaling pathway TF Su(H) is required for differentially regulating appropriate enhancer activities in PCs, and is crucial for mediating the lineage decision between PCs and CCs.

DISCUSSION

In this study, we used machine learning with DNA motifs and relevant array-based ChIP data to computationally classify cell type-specific *Drosophila* cardiac enhancers. We show that 48.7% of tested low FPR predictions with a classifier built solely on the presence of DNA motifs are active in the heart. This result is much better than one we had previously obtained for a similar classifier built to uncover muscle founder cell (FC) enhancers (Busser et al., 2012a), and may reflect a larger training set with activity restricted to the heart, a more limited number of distinct cell states for the heart compared with FCs, and/or the sequence features discriminating cardiac cell types being more unique than those for FCs (Busser et al., 2012a). In support of the latter possibility, the accuracy of *Drosophila* cardiac predictions in the present study is more consistent with our prior classification of human heart enhancers (Narlikar et al., 2010), which are likely to be subject to similar transcriptional regulatory mechanisms (Bodmer and Frasch, 2010).

Our large-scale testing of predicted enhancers also reveals the importance of ChIP data in improving enhancer modeling for cell type-specific predictions. Of note, the ChIP data for Twi, Tin and
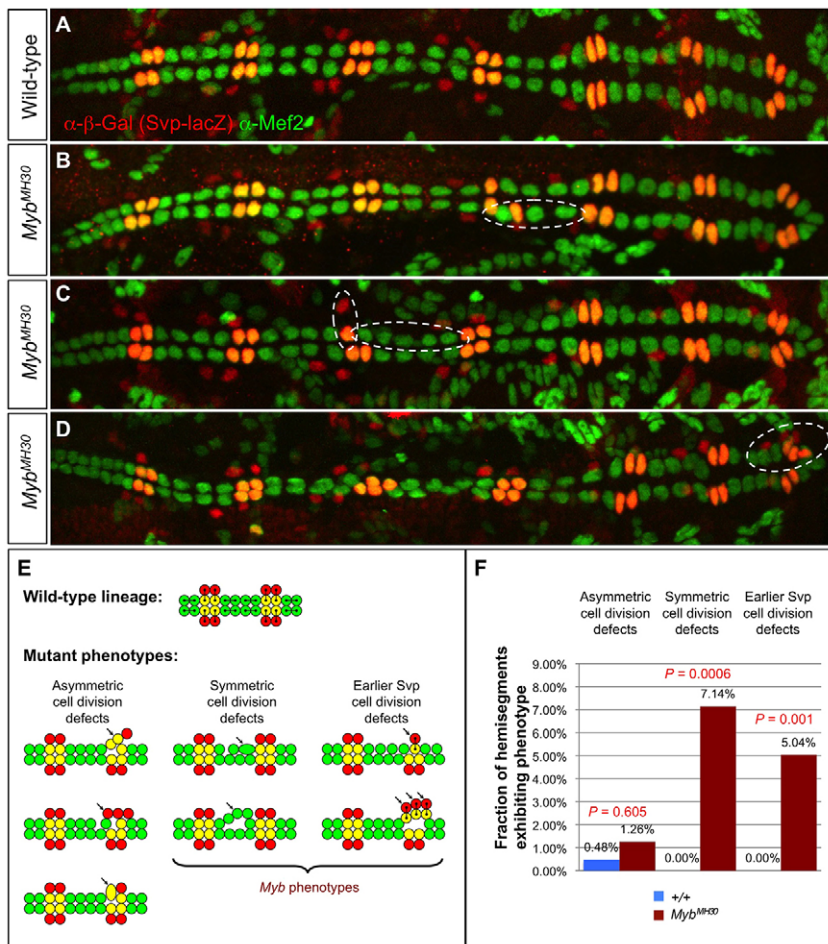
Fig. 6. Cardiac progenitor cell division defects associated with *Myb* loss of function. (A) A heart from a wild-type embryo bearing the *svp-lacZ* enhancer trap showing hemisegments consisting of four Tin-CCs (green), two Svp-CCs (yellow) and two Svp-PCs (red). (B-D) Hearts from embryos that are hemizygous for the *Myb^MH30* null mutation demonstrating mutant hemisegments with either excess or too few CCs (dashed ovals) and illustrating the two distinct types of progenitor cell division defects that underlie these cardiac phenotypes. (E) Schematic showing cell lineage relationships in a wild-type heart, and the three previously characterized cardiac progenitor cell divisions defects known to be responsible for localized changes in heart cell number (Ahmad et al., 2012). Note that only two types of developmental errors, those involved in symmetric cell divisions and those involved in an earlier step to determine the number of Svp progenitors, are primarily responsible for the *Myb* cardiac phenotypes. (F) Fraction of hemisegments exhibiting each type of cardiac progenitor cell division defect in embryos that are wild type or hemizygous for the *Myb^MH30* mutation. The significance of each type of cell division defect in the *Myb* mutants compared with wild-type embryos is shown.

Mef2 used in this study are not specific solely for cardiac cell types; these TFs are broadly expressed throughout the mesoderm, are involved in the development of numerous types of muscles, and thus bind to a wide range of mesodermal/muscle enhancers. The observation that these non-cell type-specific ChIP data are nevertheless able to significantly improve enhancer predictions specific to particular cardiac cell types suggests that our machine learning procedure is readily applicable to other systems for which ChIP data are available primarily for TFs expressed in multiple cell types.

As both Tin and Mef2 are known to confer both general and subtype properties on mesodermal cells, this latter function of these two TFs may be the crucial determinant for discovering cell type-specific predictions (Bodmer and Frasch, 2010). For example, Mef2 expression is restricted to the CCs in the differentiated heart and Tin expression is restricted to subsets of CCs and PCs. Thus, defining the *in vivo* binding profile for additional cell-specific regulators of cardiogenesis should vastly improve cell type-specific predictions, as we observed. Moreover, further refinements of our research strategy could lead to the discovery of additional features of the transcriptional codes that regulate the diversity of PC and CC subtypes (Bodmer and Frasch, 2010).

Finally, the inclusion of ChIP data significantly improved the quality of some successful enhancer predictions, as certain predictions that relied solely on motifs as discriminating features did not fall within low FPR cutoffs. This finding suggests that a unique set of sequence features are probably discriminating such enhancers, which supports the conclusion that the currently available training set of PC and CC enhancer sequences may not completely reflect the diversity of transcriptional codes that direct such enhancer activities (Busser et al., 2012a). Therefore, an iterative application of cell-specific enhancer modeling with both the training set and the newly discovered enhancer sequences is likely to improve the reliability of such predictions.

A subnetwork of two forkhead proteins, Polo kinase and Myb9 regulates cardiac progenitor cell divisions

Our previous work revealed that two forkhead TF-encoding genes, *jumu* and *CHES-1-like*, ensure the correct number of both CCs and PCs in the heart by regulating Polo activity to mediate three distinct classes of cardiac progenitor cell divisions: asymmetric cell divisions, symmetric cell divisions, and cell divisions occurring at an earlier developmental stage that generate Svp progenitor cells (Ahmad et al., 2012). In the present study, we identify another TF-encoding gene, *Myb*, which works in concert with *jumu*, *CHES-1-like* and *polo* to mediate the two latter classes of cardiac progenitor cell divisions. As *Drosophila Myb* was previously shown to regulate the expression of *polo* in a different context (Wen et al., 2008), a plausible model that both illustrates and explains our observations is presented in Fig. 8A. Consistent with this model's interpretation of the interconnected roles of *Myb*, *jumu*, *CHES-1-like* and *polo* in governing specific subsets of cardiac progenitor cell divisions, the loss of function of any one of these genes also results in abnormal spindles (Moutinho-Santos et al., 1999; Goshima et al., 2007; Wen et al., 2008), which could account for both the observed karyokinesis defects and the increase in CCs.
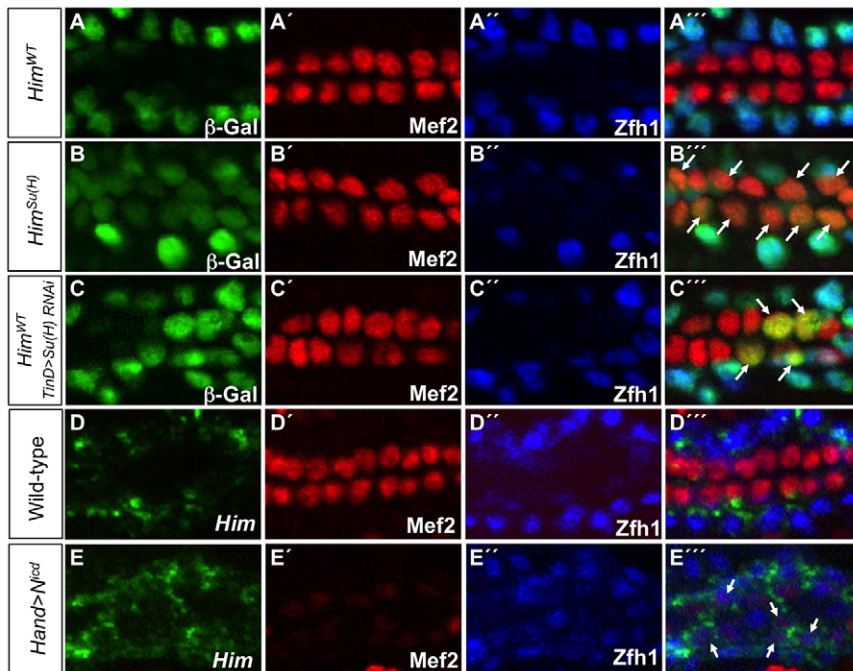
Fig. 7. Su(H) discriminates between PC and CC enhancer activities. (A-C‴) *lacZ* reporter gene activity (β-galactosidase, green) driven by relevant *Him* enhancers in indicated genotypes. All CCs express Mef2 (red) whereas PCs are marked by Zfh1 (blue). (A-A‴) The wild-type *Him* enhancer (*Him^WT*) is active only in the Zfh1-expressing PCs. (B-B‴) When the Su(H) binding site is mutated in the *Him* enhancer [*Him^Su(H)*], the reporter is still active in Zfh1-expressing PCs but is de-repressed in Mef2-positive CCs (arrows). (C-C‴) Knockdown of Su(H) with dorsal mesoderm-targeted RNAi driven by the *TinD-GAL4* driver induces ectopic *Him^WT* enhancer-driven β-galactosidase reporter activity in CCs (arrows). (D-E‴) Fluorescent *in situ* hybridization analysis of stage 16 embryos for *Him* mRNA (D,E) and antibody analysis for Mef2 (D′,E′) and Zfh1 (D″,E″) of the indicated genotypes. (D-D‴) *Him* mRNA is restricted to the Zfh1-expressing PCs of the wild-type heart. (E-E‴) Overexpression of N^icd in all cells of the heart driven by the *Hand-GAL4* driver leads to ectopic *Him* mRNA being expressed in the weakly Mef2-expressing CCs (arrows).

Given that the regulation of *polo* by the forkhead genes is also crucial for the asymmetric cell division of cardiac progenitors, an intriguing question is why *Myb*, a known regulator of *polo*, does not appear to be involved in this process. One possible explanation might be a requirement for the regulation of other components of asymmetric cell division in addition to *polo*. In this context, it is worth noting that the forkhead genes do indeed regulate additional genes involved in asymmetric cell division; for example, ectopic overexpression of *jumu* in the mesoderm results in the transcriptional upregulation of *abnormal spindle* and *Inner centromere protein* (Ahmad et al., 2012).

The Notch-dependent signaling pathway TF Su(H) discriminates between PC and CC enhancer activities

Another notable TF identified by our machine learning classifier study of *Drosophila* heart enhancers is Su(H), an integral component of the Notch signaling pathway the presence of which we found unexpectedly discriminates between PC and CC regulatory elements. Previous work had shown that in the absence of Notch signaling, co-repressors such as Groucho or C-terminal binding protein associate with Su(H) to form a repressor complex that binds to the enhancers of target genes to prevent their transcription (Bray and Furriols, 2001; Barolo and Posakony, 2002; Bray and Bernard, 2010). The activation of Notch receptors by ligand binding results in a proteolytic cleavage that releases N^icd from the cell membrane, allowing it to enter the nucleus where it associates with Su(H), displaces the co-repressor and converts the Su(H) complex from a transcriptional repressor into an activator.

The motif preferences associated with PC and CC enhancer classifications in the present study revealed an enrichment of Su(H) binding sites among PC enhancers, and either depletion or nondiscrimination among CC enhancers. We also showed that either mutating Su(H) binding motifs in the *Him* PC enhancer or reducing Su(H) levels by RNAi knockdown causes this enhancer to drive expression ectopically in CCs, implying that Su(H) normally represses *Him* in CCs. Finally, we showed that ectopically expressing N^icd in both CCs and PCs results in de-repression of the

Him transcript in CCs, demonstrating that Notch signaling activates this PC gene. As we describe below, these studies confirm a requirement of Su(H) binding sites for restricting enhancer activity to PCs.

These results are in agreement with previous investigations of the role of Notch function in cardiogenesis. For example, inactivating mutations of *Notch* or *Delta*, the relevant ligand for Notch in cardiogenesis, lead to an overproduction of CCs at the expense of PCs (Mandal et al., 2004; Grigorian et al., 2011), thus indicating a role for Notch signaling in activating key PC genes, whereas relieving the antagonism of Notch signaling through *numb* loss-of-function mutations results in additional PCs at the expense of CCs (Gajewski et al., 2000; Ward and Skeath, 2000; Han and Olson, 2005). Interestingly, a recent study has shown that Delta expression is restricted to CCs (Grigorian et al., 2011), suggesting that cell-cell signaling between CC and PC progenitors is crucial for the proper restriction of cell fates in the CM, a result consistent with the trans-activating role of Notch (Niessen and Karsan, 2008). Furthermore, the cardiogenic functions of Notch signaling are conserved in vertebrates, as this pathway is involved in the differentiation and proliferation of cardiomyocytes as well as in the formation of the atrioventricular canal and the outflow tract (Niessen and Karsan, 2008). Collectively, these results suggest that Notch signaling mediated by progenitors fated to become CCs instructs nearby progenitors to assume the PC fate, a process that is in part mediated by Su(H) directly regulating key PC target genes. A model that synthesizes and explains the entirety of our observations on Notch-Su(H) regulation of cardiogenesis is presented in Fig. 8B and supplementary material Fig. S10A-D.

Conclusions

Here, we combined sequence features with ChIP data for key cardiac regulators to computationally classify cell type-specific *Drosophila* cardiac enhancers, thereby identifying heart regulatory elements on a genome-wide scale, their shared and unique sequence motifs, and novel TFs that direct cell type-specific genetic programs during cardiogenesis. Illustrative examples of
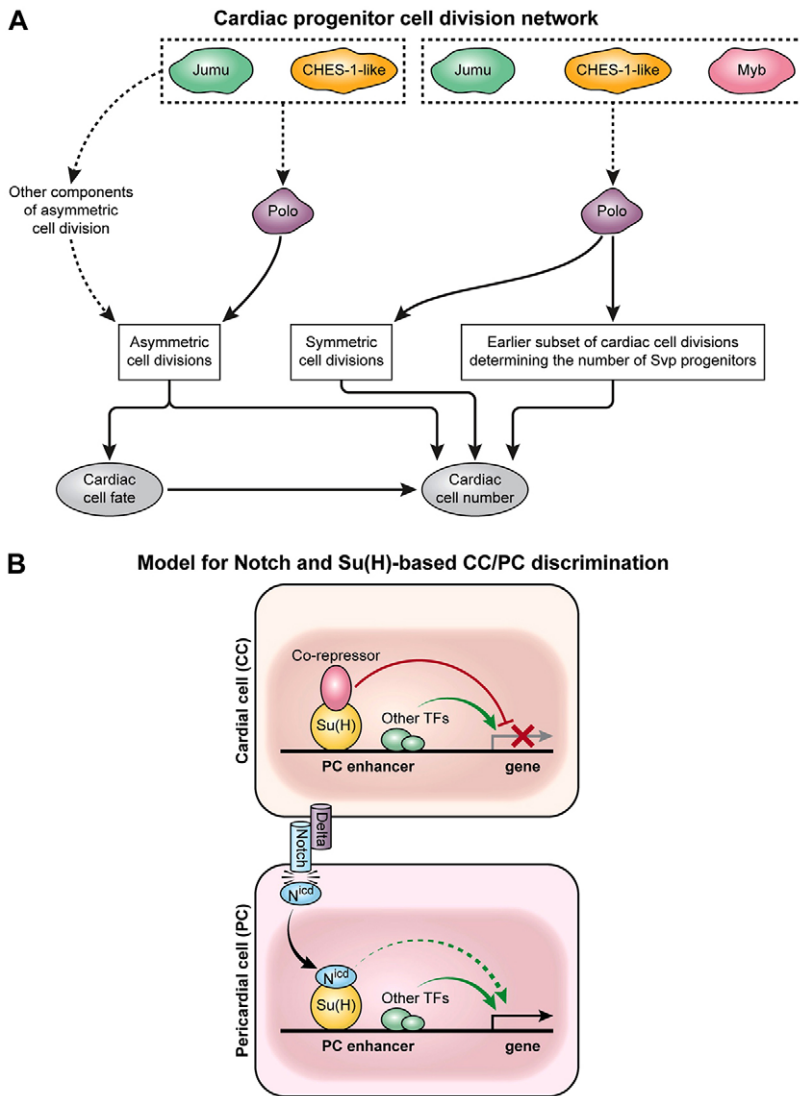
Fig. 8. Distinct developmental subnetworks regulate cardiac progenitor cell division and specification.
(A) Schematic of Jumu, CHES-1-like and Myb regulation of cardiac progenitor cell divisions by Polo kinase. The forkhead TFs Jumu and CHES-1-like regulate Polo kinase activity to mediate three distinct classes of cardiac progenitor cell divisions: asymmetric cell divisions, symmetric cell divisions, and an earlier round of cell division that determines the number of Svp progenitors (Ahmad et al., 2012). Mutations in *Myb* result in defects in only the latter two categories of cell divisions, which also exhibit synergistic genetic interactions among *Myb*, *jumu*, *CHES-1-like* and *polo*. As Myb transcriptionally regulates *polo* (Wen et al., 2008), Myb and the forkhead TFs act in concert to control Polo activity and thus govern both the symmetric and earlier class of cell divisions. (B) Schematic of the involvement of the Notch signaling pathway in the lineage decision between PCs and CCs for PC enhancers like that of *Him*. Modes of regulation activating and repressing target genes are shown as green and red arrows, respectively. In CCs, the enhancers of PC genes are repressed by the Su(H)-co-repressor complex. The Delta ligand expressed by CCs activates Notch receptor in neighboring PCs, with the resulting cleaved N^{icd} fragment associating with Su(H) and displacing the co-repressor. The consequent elimination of repressor complex binding in PCs is sufficient to initiate transcription due to the presence of other local TF activators, and is enhanced further by the N^{icd}-Su(H) complex.

these computational predictions were validated by appropriate *in vivo* experiments. The combination of computational and experimental approaches that we employed are generalizable and should readily be applicable to augment an understanding of the developmental gene regulatory networks that operate in other cell types and species.

MATERIALS AND METHODS
Fly stocks and analysis of transgenic reporter constructs
The analysis of site-specific transgenic reporter constructs, antibodies and fly stocks used in this study were previously described (Manak et al., 2002; Ahmad et al., 2012; Busser et al., 2012c; Busser et al., 2012b; Busser et al., 2012a).

Identification and mutagenesis of TF binding sites
Su(H) binding sites were identified by searching sequences for matches to YGTGDGAA (while omitting matches to TGTGTGAA), and single-base mutations were engineered to abrogate Su(H) binding in otherwise wild-type enhancers, as documented in a prior study (Rebeiz et al., 2011). Mutagenesis of the Myb binding sites in the *Ndg* enhancer was previously described (Busser et al., 2012a).

Classifier training
The methodology behind the isolation of orthologous and control sequences, development of sequence-based classifiers, genome-wide prediction of

enhancers, and association of cell-specific genes with predicted enhancers was previously described (Busser et al., 2012a). The full dataset has been deposited at Figshare in the form of an extended version of supplementary material Table S2 (http://dx.doi.org/10.6084/m9.figshare.867687).

Author contributions
B.W.B., D.H., I.O. and A.M.M. designed the overall research project. S.M.A. and B.W.B. designed individual experiments and interpreted the results. S.M.A., B.W.B., D.H., I.O. and A.M.M. wrote the manuscript. B.W.B., E.J.C. and X.Z. performed transgenic reporter assays. D.H. and I.O. constructed classifiers and performed related statistical analyses. S.M.A., X.Z., S.M. and B.W.B. performed *cis* tests of *Ndg* and *Him* enhancer function. S.M.A. performed *trans* tests of *Ndg* and *Him* enhancer function and genetic interaction studies. A.A. and M.L.B. contributed data/materials/analysis tools. N.J. performed *Myb*-related statistical analyses.

Supplementary material

Supplementary material available online at
http://dev.biologists.org/lookup/suppl/doi:10.1242/dev.101709/-/DC1

References

Ahmad, S. M., Tansey, T. R., Busser, B. W., Nolte, M. T., Jeffries, N., Gisselbrecht, S. S., Rusan, N. M. and Michelson, A. M. (2012). Two forkhead transcription factors regulate the division of cardiac progenitor cells by a Polo-dependent pathway. *Dev. Cell* 23, 97-111.

Bailey, T. L. and Gribskov, M. (1998). Combining evidence using p-values: application to sequence homology searches. *Bioinformatics* 14, 48-54.

Barolo, S. and Posakony, J. W. (2002). Three habits of highly effective signaling pathways: principles of transcriptional control by developmental cell signaling. *Genes Dev.* 16, 1167-1181.

Berger, M. F., Philippakis, A. A., Qureshi, A. M., He, F. S., Estep, P. W., III and Bulyk, M. L. (2006). Compact, universal DNA microarrays to comprehensively determine transcription-factor binding site specificities. *Nat. Biotechnol.* 24, 1429-1435.

Bernard, F., Krejci, A., Housden, B., Adryan, B. and Bray, S. J. (2010). Specificity of Notch pathway activation: twist controls the transcriptional output in adult muscle progenitors. *Development* 137, 2633-2642.

Bodmer, R. and Frasch, M. (2010). Development and aging of the Drosophila heart. In *Heart Development and Regeneration* (ed. N. Rosenthal and R. P. Harvey). London: Academic Press.

Bray, S. and Bernard, F. (2010). Notch targets and their regulation. *Curr. Top. Dev. Biol.* 92, 253-275.

Bray, S. and Furriols, M. (2001). Notch pathway: making sense of suppressor of hairless. *Curr. Biol.* 11, R217-R221.

Busser, B. W., Bulyk, M. L. and Michelson, A. M. (2008). Toward a systems-level understanding of developmental regulatory networks. *Curr. Opin. Genet. Dev.* 18, 521-529.

Busser, B. W., Taher, L., Kim, Y., Tansey, T., Bloom, M. J., Ovcharenko, I. and Michelson, A. M. (2012a). A machine learning approach for identifying novel cell type-specific transcriptional regulators of myogenesis. *PLoS Genet.* 8, e1002531.

Busser, B. W., Shokri, L., Jaeger, S. A., Gisselbrecht, S. S., Singhania, A., Berger, M. F., Zhou, B., Bulyk, M. L. and Michelson, A. M. (2012b). Molecular mechanism underlying the regulatory specificity of a Drosophila homeodomain protein that specifies myoblast identity. *Development* 139, 1164-1174.

Busser, B. W., Huang, D., Rogacki, K. R., Lane, E. A., Shokri, L., Ni, T., Gamble, C. E., Gisselbrecht, S. S., Zhu, J., Bulyk, M. L. et al. (2012c). Integrative analysis of the zinc finger transcription factor Lame duck in the Drosophila myogenic gene regulatory network. *Proc. Natl. Acad. Sci. USA* 109, 20768-20773.

Chang, C. C. and Lin, C. J. (2011). LIBSVM: A library for support vector machines. *ACM Transactions on Intelligent Systems and Technology* 2, 27.

Cortes, C. and Vapnik, V. (1995). Support-vector networks. *Mach. Learn.* 20, 273-297.

Davidson, E. (2006). *The Regulatory Genome: Gene Regulatory Networks in Development And Evolution*. London: Academic Press.

Davison, A. and Hinkley, D. (1997). *Bootstrap Methods and Their Application*. Cambridge: Cambridge University Press.

DeBruhl, H., Wen, H. and Lipsick, J. S. (2013). The complex containing Drosophila Myb and RB/E2F2 regulates cytokinesis in a histone H2Av-dependent manner. *Mol. Cell. Biol.* 33, 1809-1818.

Gajewski, K., Choi, C. Y., Kim, Y. and Schulz, R. A. (2000). Genetically distinct cardial cells within the Drosophila heart. *Genesis* 28, 36-43.

Good, P. (1994). *Permutation Tests: a Practical Guide to Resampling Methods for Testing Hypotheses*. New York, NY: Springer-Verlag.

Goshima, G., Wollman, R., Goodwin, S. S., Zhang, N., Scholey, J. M., Vale, R. D. and Stuurman, N. (2007). Genes required for mitotic spindle assembly in Drosophila S2 cells. *Science* 316, 417-421.

Grigorian, M., Mandal, L., Hakimi, M., Ortiz, I. and Hartenstein, V. (2011). The convergence of Notch and MAPK signaling specifies the blood progenitor fate in the Drosophila mesoderm. *Dev. Biol.* 353, 105-118.

Han, Z. and Olson, E. N. (2005). Hand is a direct target of Tinman and GATA factors during Drosophila cardiogenesis and hematopoiesis. *Development* 132, 3525-3536.

Jin, H., Stojnic, R., Adryan, B., Ozdemir, A., Stathopoulos, A. and Frasch, M. (2013). Genome-wide screens for in vivo Tinman binding sites identify cardiac enhancers with diverse functional architectures. *PLoS Genet.* 9, e1003195.

Johnson, A. N., Mokalled, M. H., Haden, T. N. and Olson, E. N. (2011). JAK/Stat signaling regulates heart precursor diversification in Drosophila. *Development* 138, 4627-4638.

Junion, G., Spivakov, M., Girardot, C., Braun, M., Gustafson, E. H., Birney, E. and Furlong, E. E. (2012). A transcription factor collective defines cardiac cell fate and reflects lineage history. *Cell* 148, 473-486.

Kantorovitz, M. R., Kazemian, M., Kinston, S., Miranda-Saavedra, D., Zhu, Q., Robinson, G. E., Göttgens, B., Halfon, M. S. and Sinha, S. (2009). Motif-blind, genome-wide discovery of cis-regulatory modules in Drosophila and mouse. *Dev. Cell* 17, 568-579.

Katzen, A. L., Jackson, J., Harmon, B. P., Fung, S. M., Ramsay, G. and Bishop, J. M. (1998). Drosophila myb is required for the G2/M transition and maintenance of diploidy. *Genes Dev.* 12, 831-843.

Krejcí, A., Bernard, F., Housden, B. E., Collins, S. and Bray, S. J. (2009). Direct response to Notch activation: signaling crosstalk and incoherent logic. *Sci. Signal.* 2, ra1.

Liu, Y. H., Jakobsen, J. S., Valentin, G., Amarantos, I., Gilmour, D. T. and Furlong, E. E. (2009). A systematic analysis of Tinman function reveals Eya and JAK-STAT signaling as essential regulators of muscle development. *Dev. Cell* 16, 280-291.

Manak, J. R., Mitiku, N. and Lipsick, J. S. (2002). Mutation of the Drosophila homologue of the Myb protooncogene causes genomic instability. *Proc. Natl. Acad. Sci. USA* 99, 7438-7443.

Mandal, L., Banerjee, U. and Hartenstein, V. (2004). Evidence for a fruit fly hemangioblast and similarities between lymph-gland hematopoiesis in fruit fly and mammal aorta-gonadal-mesonephros mesoderm. *Nat. Genet.* 36, 1019-1023.

Moutinho-Santos, T., Sampaio, P., Amorim, I., Costa, M. and Sunkel, C. E. (1999). In vivo localisation of the mitotic POLO kinase shows a highly dynamic association with the mitotic apparatus during early embryogenesis in Drosophila. *Biol. Cell* 91, 585-596.

Narlikar, L., Sakabe, N. J., Blanski, A. A., Arimura, F. E., Westlund, J. M., Nobrega, M. A. and Ovcharenko, I. (2010). Genome-wide discovery of human heart enhancers. *Genome Res.* 20, 381-392.

Niessen, K. and Karsan, A. (2008). Notch signaling in cardiac development. *Circ. Res.* 102, 1169-1181.

Olson, E. N. (2006). Gene regulatory networks in the evolution and development of the heart. *Science* 313, 1922-1927.

Park, M., Yaich, L. E. and Bodmer, R. (1998). Mesodermal cell fate decisions in *Drosophila* are under the control of the lineage genes *numb*, *Notch*, and *sanpodo*. *Mech. Dev.* 75, 117-126.

Philippakis, A. A., Busser, B. W., Gisselbrecht, S. S., He, F. S., Estrada, B., Michelson, A. M. and Bulyk, M. L. (2006). Expression-guided in silico evaluation of candidate cis regulatory codes for Drosophila muscle founder cells. *PLOS Comput. Biol.* 2, e53.

Ramsay, R. G. (2005). c-Myb a stem-progenitor cell regulator in multiple tissue compartments. *Growth Factors* 23, 253-261.

Rebeiz, M., Miller, S. W. and Posakony, J. W. (2011). Notch regulates numb: integration of conditional and autonomous cell fate specification. *Development* 138, 215-225.

Sandelin, A., Alkema, W., Engström, P., Wasserman, W. W. and Lenhard, B. (2004). JASPAR: an open-access database for eukaryotic transcription factor binding profiles. *Nucleic Acids Res.* 32, D91-D94.

Tomancak, P., Berman, B. P., Beaton, A., Weiszmann, R., Kwan, E., Hartenstein, V., Celniker, S. E. and Rubin, G. M. (2007). Global analysis of patterns of gene expression during Drosophila embryogenesis. *Genome Biol.* 8, R145.

Ward, E. J. and Skeath, J. B. (2000). Characterization of a novel subset of cardiac cells and their progenitors in the Drosophila embryo. *Development* 127, 4959-4969.

Warner, J. B., Philippakis, A. A., Jaeger, S. A., He, F. S., Lin, J. and Bulyk, M. L. (2008). Systematic identification of mammalian regulatory motifs' target genes and functions. *Nat. Methods* 5, 347-353.

Wen, H., Andrejka, L., Ashton, J., Karess, R. and Lipsick, J. S. (2008). Epigenetic regulation of gene expression by Drosophila Myb and E2F2-RBF via the Myb-MuvB/dREAM complex. *Genes Dev.* 22, 601-614.

Wingender, E., Chen, X., Fricke, E., Geffers, R., Hehl, R., Liebich, I., Krull, M., Matys, V., Michael, H., Ohnhäuser, R. et al. (2001). The TRANSFAC system on gene expression regulation. *Nucleic Acids Res.* 29, 281-283.

Yin, Z., Xu, X. L. and Frasch, M. (1997). Regulation of the twist target gene tinman by modular cis-regulatory elements during early mesoderm development. *Development* 124, 4971-4982.

Zhu, X., Ahmad, S. M., Aboukhalil, A., Busser, B. W., Kim, Y., Tansey, T. R., Haimovich, A., Jeffries, N., Bulyk, M. L. and Michelson, A. M. (2012). Differential regulation of mesodermal gene expression by Drosophila cell type-specific Forkhead transcription factors. *Development* 139, 1457-1466.

Zinzen, R. P., Girardot, C., Gagneur, J., Braun, M. and Furlong, E. E. (2009). Combinatorial binding predicts spatio-temporal cis-regulatory activity. *Nature* 462, 65-70.
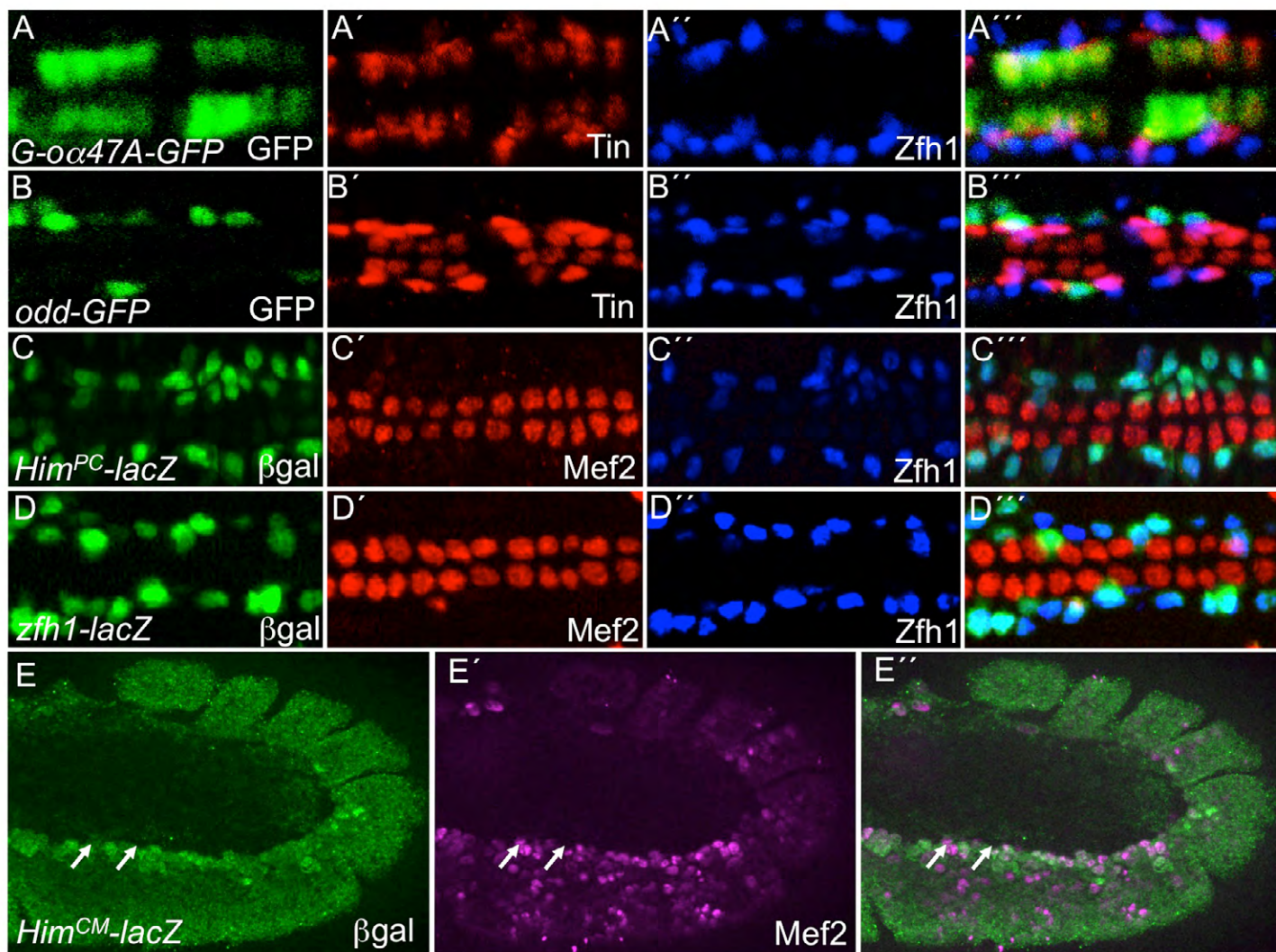
Supplementary Fig. S1. Building a training set of cardiac enhancers. (A-E) Empirical validation of candidate enhancers containing matches to Twi and Tin TFBS motifs and located in the flanking or intronic sequences associated with previously characterized heart genes (Warner et al., 2008). Enhancer coordinates are described in supplementary material Table S1. Antibody staining of stage 16 (A-D) and stage 11 (E) embryos containing *G-oα47A-GFP* (A), *odd-GFP* (B), *Him^PC^-lacZ* (C), *zfh1-lacZ* (D) and *Him^CM^-lacZ* (E) transgenes using antibodies against GFP (A,B), β-galactosidase (C-E), Tin (A-B), Mef2 (C-E) and Zfh1 (A-D). Panels A-E represent the activity of the relevant *lacZ* or *GFP* reporter, while Tin (Tin-expressing CCs and PCs), Zfh1 (all PCs) and Mef2 (all CCs) were used to stain and distinguish different cardiac cell types. *zfh1-lacZ* is active in all PCs whereas the enhancers for *G-oα47A-GFP* and *odd-GFP* are active in subsets of the PCs, with *G-oα47A-GFP* restricted to the 4 Tin-expressing PCs and *odd-GFP* is present in all of the Odd-expressing PCs. Separate enhancers control the activity of the Him gene, as *Him^PC^-lacZ* is active in all PCs at stage 16 whereas *Him^CM^-lacZ* is only active in cells of the cardiac mesoderm (arrows) at stage 11.
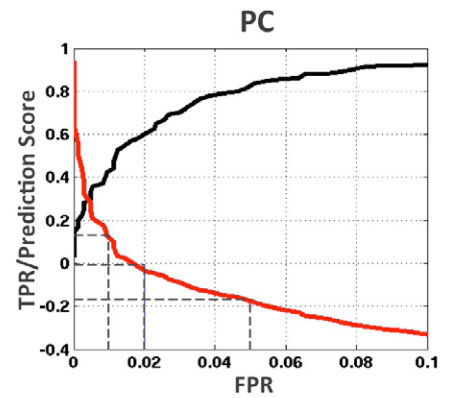
A) motif+ChIP

Heart
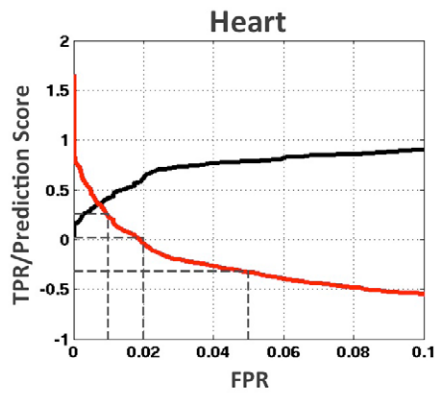
False Positive Rate	Score	Number of positive predictions
0.01	0.26	2682
0.02	0.02	5925
0.05	-0.25	12294

CC
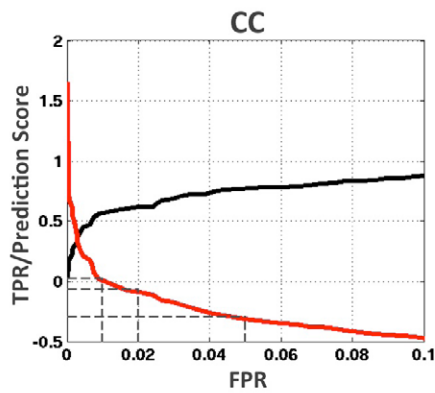
False Positive Rate	Score	Number of positive predictions
0.01	0.03	2962
0.02	-0.07	4303
0.05	-0.30	10804

PC

False Positive Rate	Score	Number of positive predictions
0.01	0.17	1907
0.02	-0.01	3330
0.05	-0.19	7124

B) motif-alone

Heart
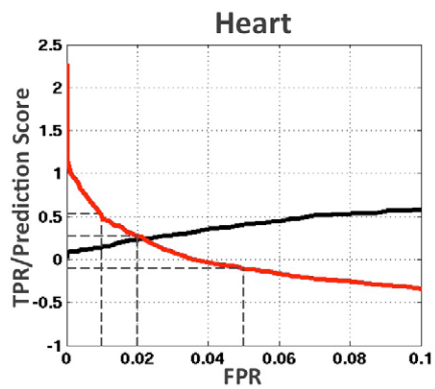
False Positive Rate	Score	Number of positive predictions
0.01	0.53	1787
0.02	0.27	4832
0.05	-0.1	9619

CC
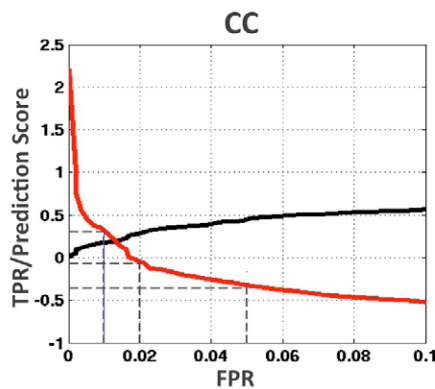
False Positive Rate	Score	Number of positive predictions
0.01	0.31	1285
0.02	-0.03	6339
0.05	-0.35	18457

PC
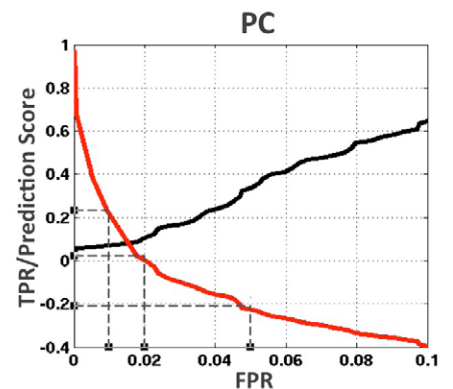
| False Positive Rate	Score	Number of positive predictions
0.01	0.22	2097
0.02	0.01	5161
0.05	-0.20	12009

Supplementary Fig. S2. Prediction of cardiac enhancers at different false positive rates (FPRs). Prediction score cutoffs and true positive rates (TPRs) were plotted for different FPRs. In the tables, three typical FPRs (i.e. 0.01, 0.02 and 0.05) and the corresponding prediction results are shown.
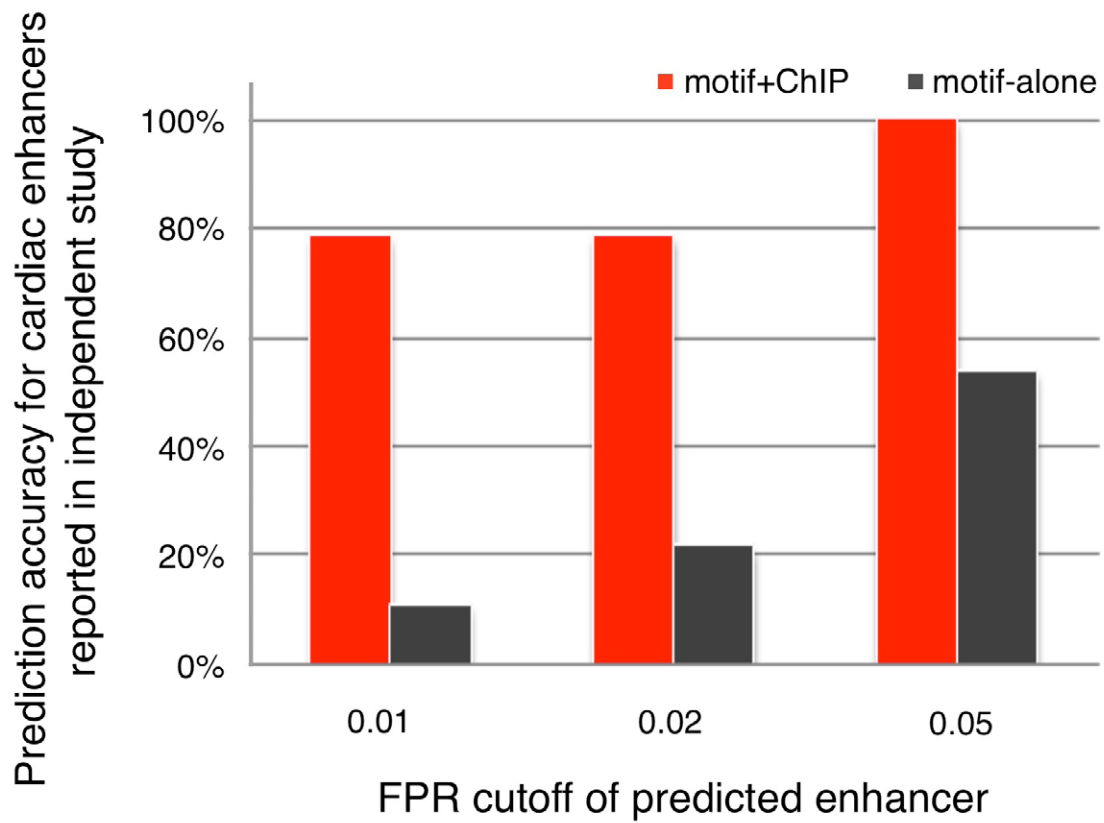
Supplementary Fig. S3. Prediction accuracy of heart classifiers for cardiac enhancers reported in an independent study. Histogram showing the fraction of *in vivo* verified cardiac enhancers from an independent study (Jin et al., 2013) that were accurately predicted by the motif+ChIP and motif-alone heart classifiers at different FPRs.
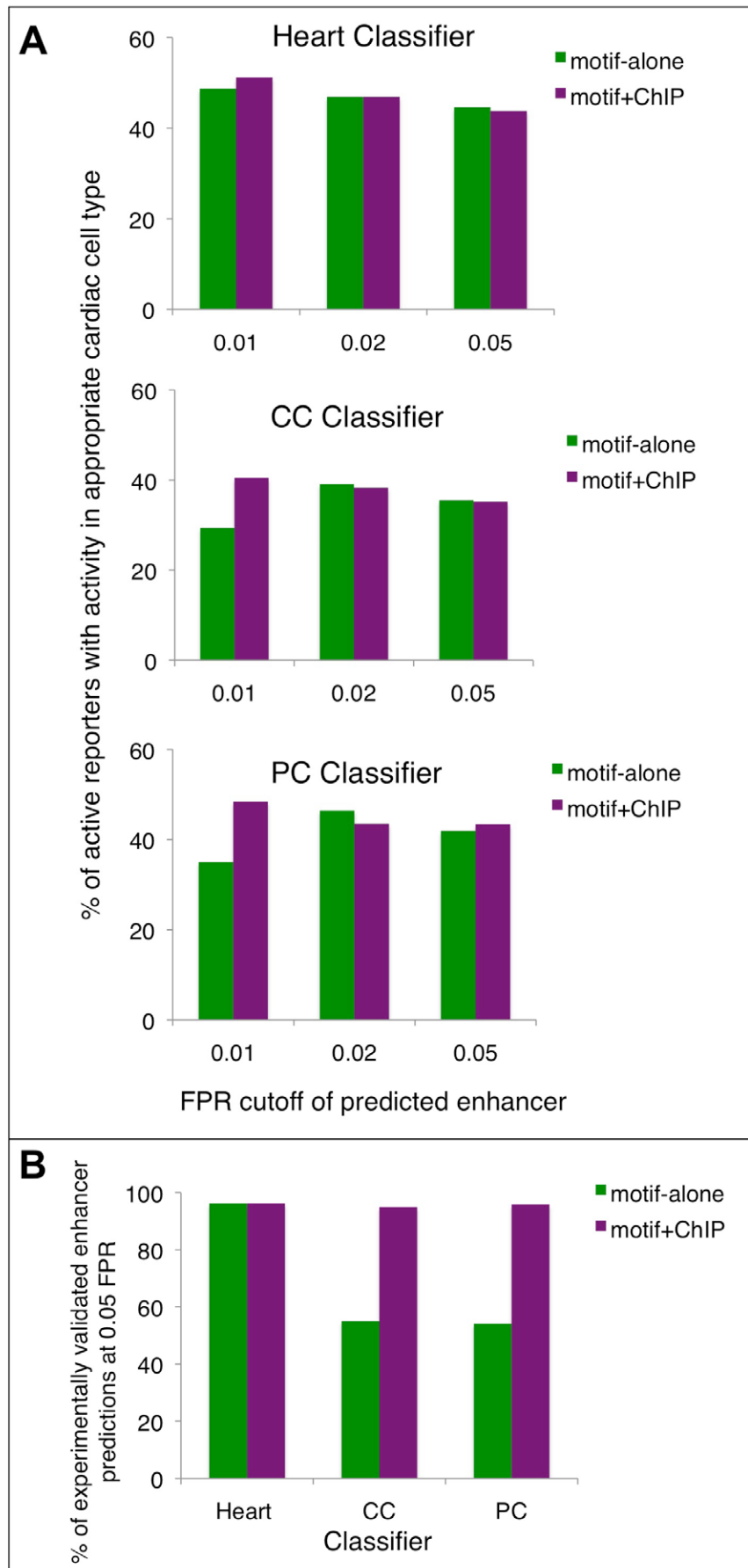
Supplementary Fig. S4. Empirical validation of classifier predictions. (A) Percentages of predicted enhancers with activity in the appropriate cardiac cell types for the motif-alone and motif+ChIP classifiers at different FPRs. (B) Percentages of successful enhancer predictions with activity in the appropriate cardiac cell types for the motif-alone and motif+ChIP classifiers at 0.05 FPR
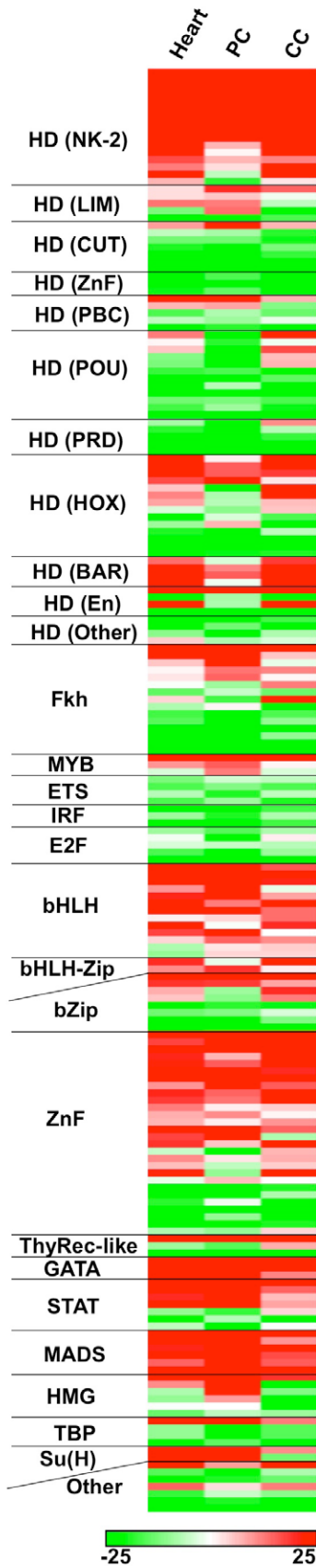
Supplementary Fig. S5. Machine learning reveals motif features associated with cardiac enhancer subtypes. A linear SVM was trained for each cardiac training set using only TF binding motifs (motif-alone classifier). Motifs are represented according to their linear SVM weights (a reflection of the discriminating power of these motifs). For each cardiac training set, the binding motifs were grouped according to the DNA-binding domain of the TF. See supplementary material Table S3 for motifs and motif weights. Similar results were seen for the motif+ChIP classifier (see Fig. 3).
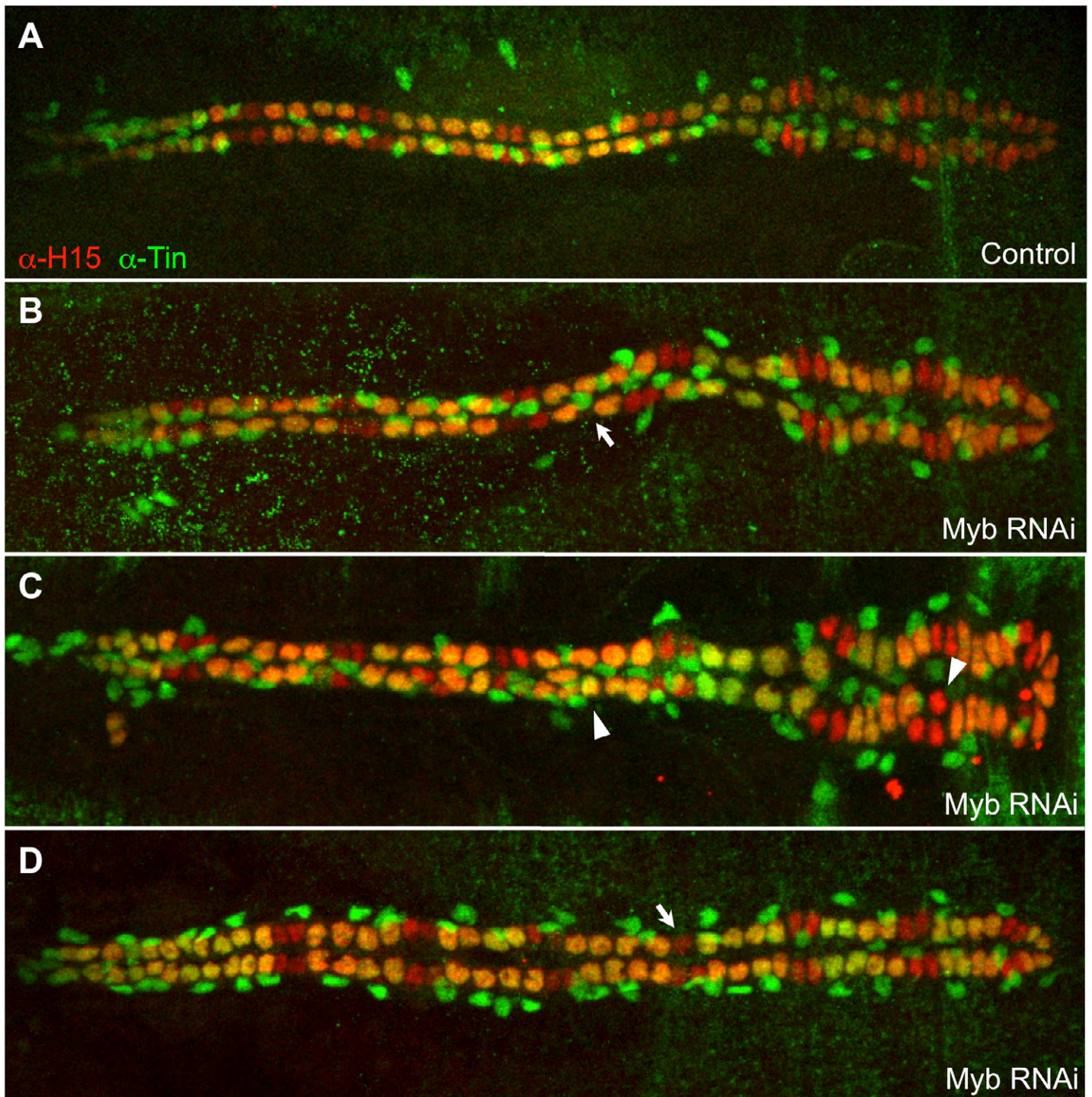
Supplementary Fig. S6. Cardiac phenotypes associated with knocking down Myb levels specifically in the developing heart using a targeted RNAi-based strategy. (A-D) Hearts from embryos stained with antibodies against Tin and with a CC-specific antibody against H15 such that Tin-CCs (yellow) can be distinguished from Svp-CCs (red). Anterior is to the left. (A) Heart from a control embryo. Note that every hemisegment except the posteriormost (A8) hemisegments includes four Tin-CCs and two Svp-CCs. (B-D) Hearts from embryos in which RNAi driven by both the cardiac-speccific drivers TinD-GAL4 and Hand-Gal4 is utilized to knock down Myb levels specifically in the developing heart. Localized reductions (arrows) in the number of both Tin-CCs (B) and Svp-CCs (D), as well as localized increases in both Tin-CCs and Svp-CCs (arrowheads in C), are detected.
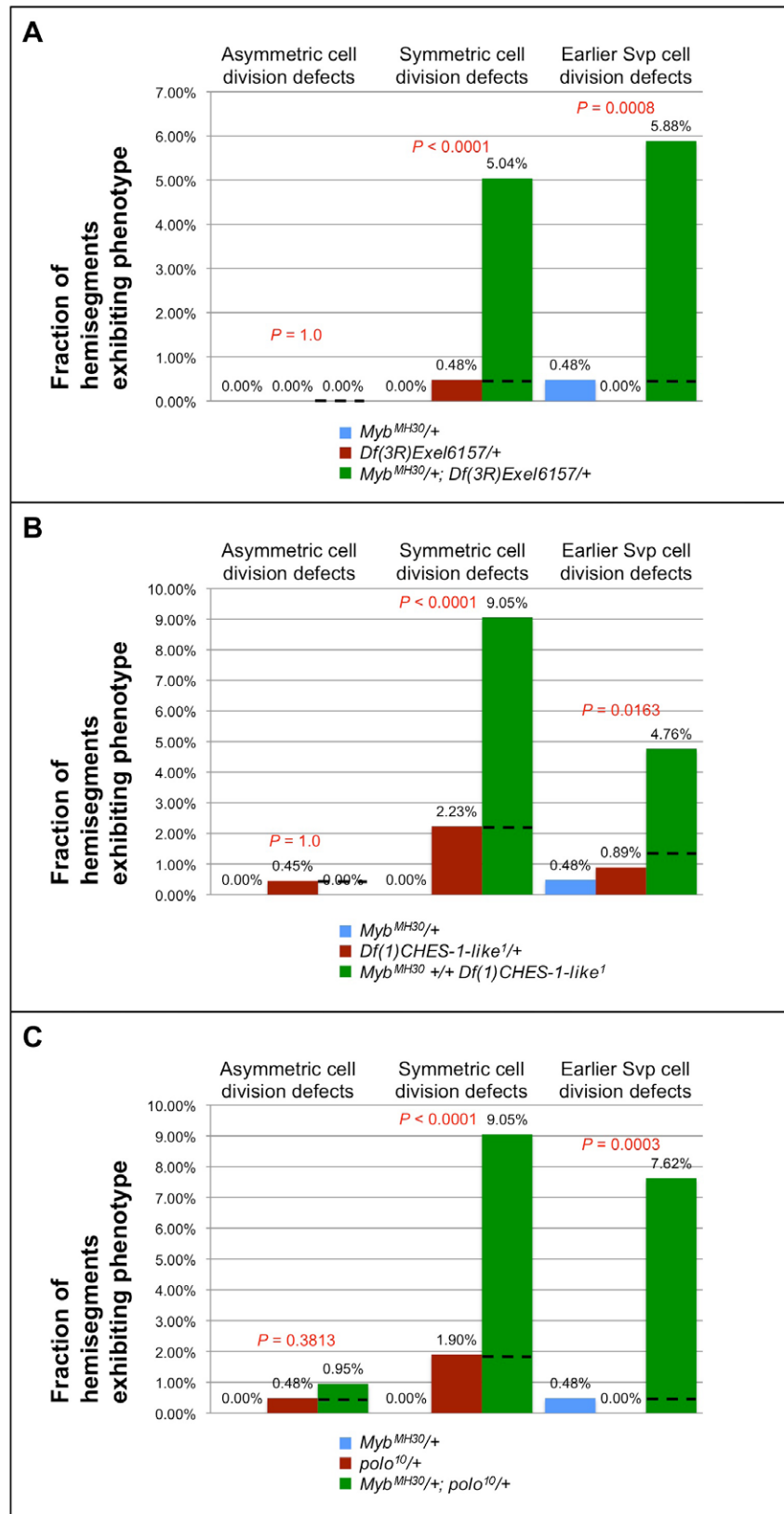
Supplementary Fig. S7. Synergistic interactions between the genes encoding Myb, Jumu, CHES-1-like and Polo proteins. (A) Fraction of hemisegments exhibiting asymmetric, symmetric, and earlier cell division defects affecting Svp progenitor numbers for single and double heterozygotes of a deficiency, *Df(3R)Exel6157*, which completely eliminates the *jumu* gene, and *Myb^MH30*, a null mutation in *Myb*. (B) Fraction of hemisegments exhibiting the three types of cardiac progenitor cell division defects for single and double heterozygotes of null mutations in *Myb* and *CHES-1-like*. (C) Fraction of hemisegments exhibiting the cardiac progenitor cell division defects for single and double heterozygotes of the *Myb* null mutation, and a strong hypomorphic mutation in *polo*. In each case, the black dashed line indicates the expected results in the double heterozygotes if the phenotypes were purely additive. See Supplementary Fig. S8 for representative images of these cardiac progenitor cell division defects.
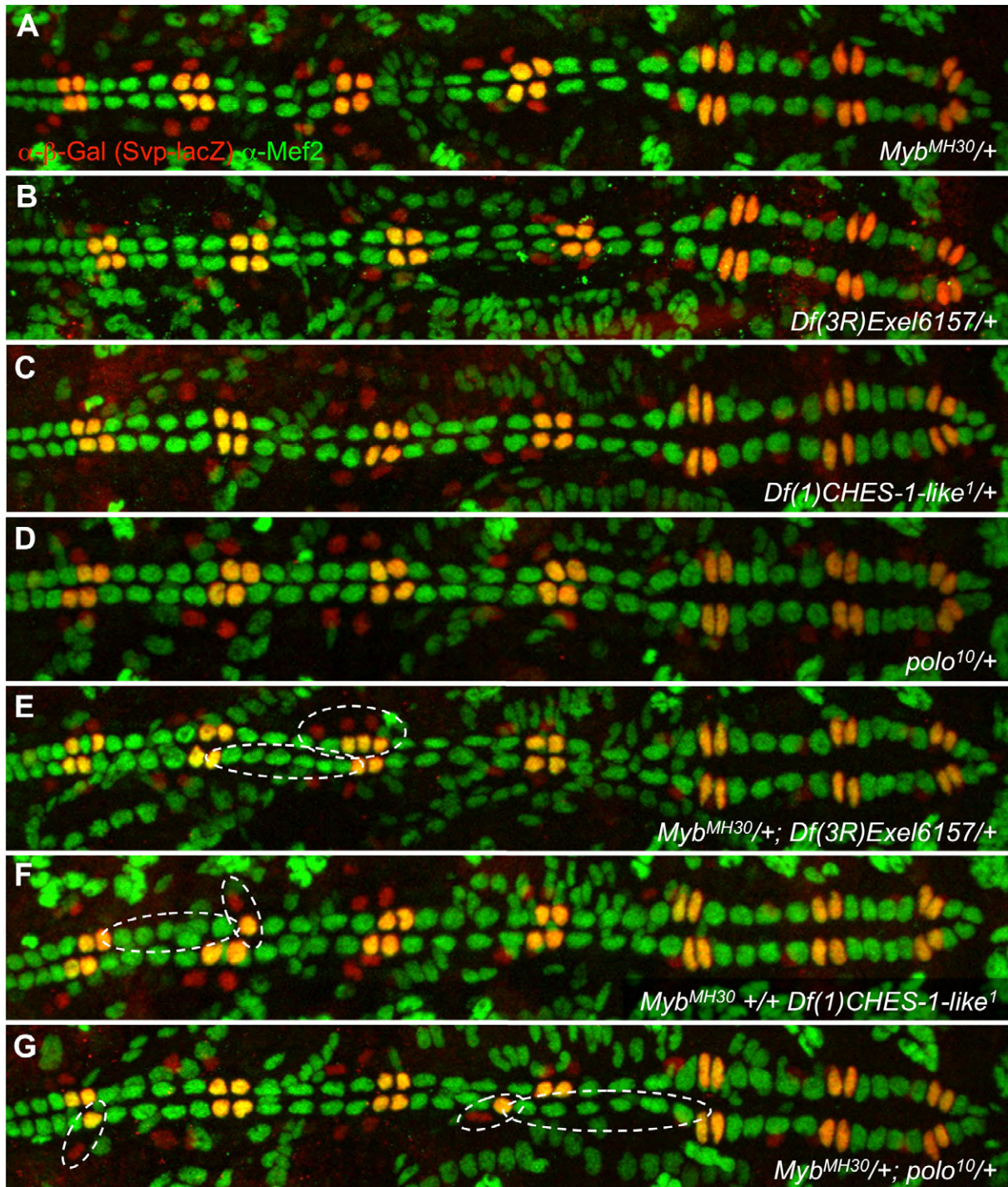
Supplementary Fig. S8. Cardiac phenotypes associated with single and double heterozygotes for mutations in *Myb*, *jumu*, *CHES-1-like* and *polo*. (A-D) Representative hearts from embryos that are individually heterozygous for a null mutation in *Myb* (A), a deficiency that completely eliminates *jumu* (B), a null mutation in *CHES-1-like* (C), or a strong hypomorphic mutation in *polo* (D) are shown. Note that these single heterozygotes typically do not exhibit cardiac progenitor cell division defects. (E-G) In contrast, representative hearts from embryos doubly heterozygous for mutations in *Myb* and either *jumu* (E), *CHES-1-like* (F) or *polo* (G) exhibit significant cardiac phenotypes (dashed ovals) associated with defects in symmetric cell division and earlier cell divisions affecting the number of Svp progenitors. See Supplementary Fig. S7 for quantitation.
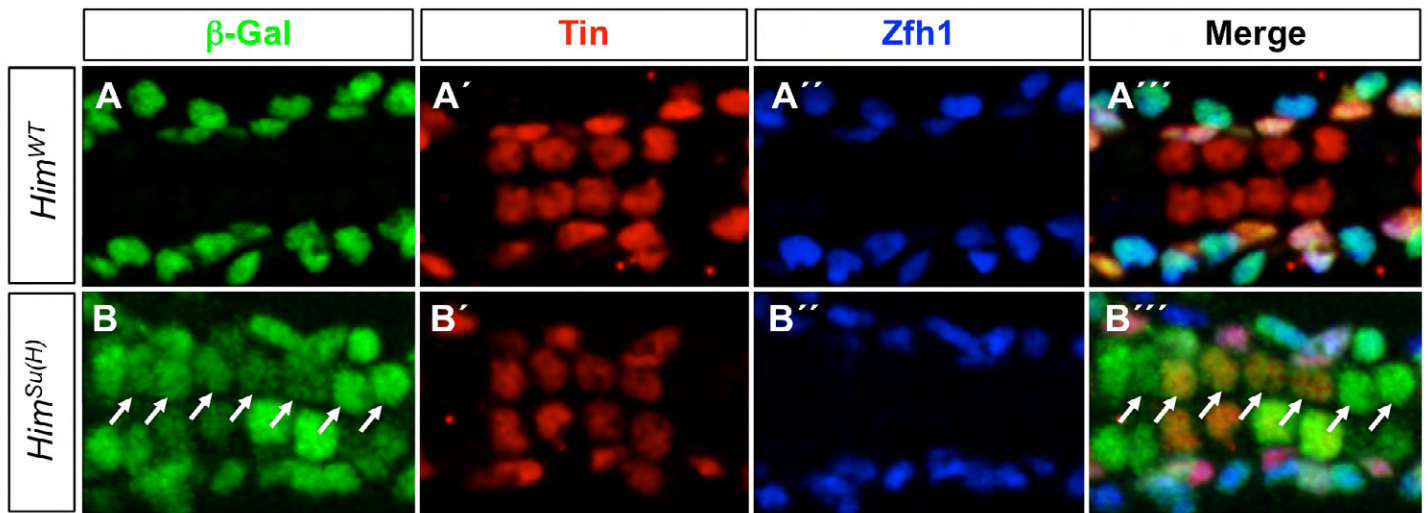
Supplementary Fig. S9. The Su(H) binding site is utilized to repress expression of the *Him* PC enhancer in CCs. The posterior-most four CCs are marked by Tin expression (red), and the PCs are marked by Zfh1 expression (blue). (A-A´´´) A β-galactosidase reporter (green) driven by the wild-type *Him* enhancer (*Him^WT^*) is expressed only in the Zfh1-expressing PCs. (B-B´´´) When the Su(H) binding site is mutated in the *Him* enhancer (*Him^Su(H)^*), the reporter is ectopically expressed in CCs (arrows). Its expression in all Zfh1-expressing PCs remains unaltered.

Model for Notch and Su(H)-based CC/PC discrimination
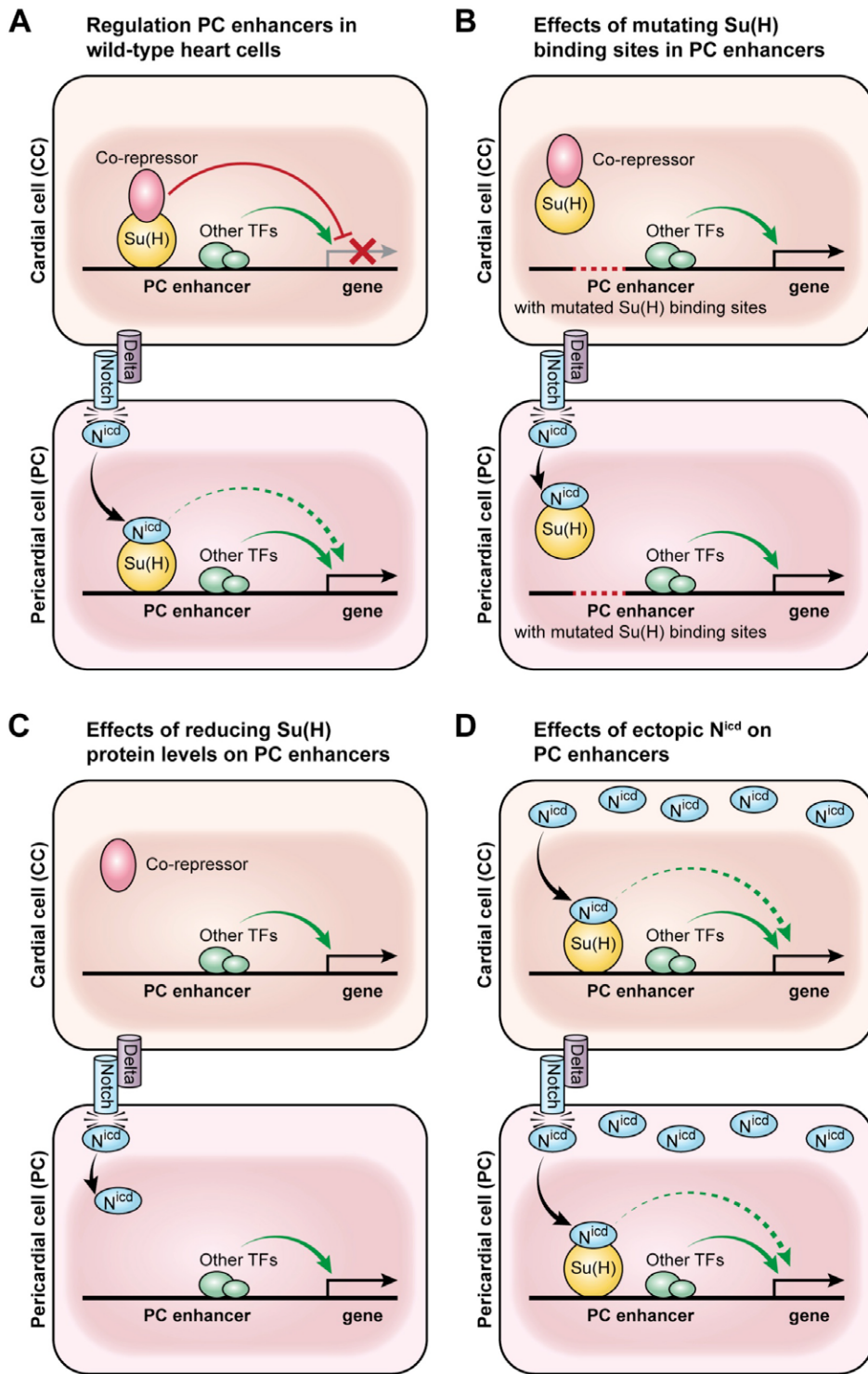
Supplementary Fig. S10. Schematic of the involvement of the Notch signaling pathway in the lineage decision between PCs and CCs for PC enhancers. Modes of regulation activating and repressing target genes are shown as green and red arrows respectively. (A) In cardial cells, the enhancers of PC genes such as *Him* are repressed by the Su(H)-co-repressor complex. The Delta ligand expressed by CCs activates Notch receptor in neighboring PCs, with the resulting cleaved N^{icd} fragment associating with Su(H) and displacing the co-repressor. The consequent elimination of repressor complex binding in PCs is sufficient to initiate transcription due to the presence of other local TF activators, which is enhanced further by the N^{icd}-Su(H) complex in PCs. (B) Mutating the Su(H) sites in PC enhancers prevents the Su(H)-co-repressor complex from binding to the enhancers in CCs. The resulting alleviation of repression is sufficient to ectopically transcribe the associated gene in CCs. (C) Similarly, minimizing the level of Su(H) protein by RNA interference reduces the formation and subsequent binding of the Su(H)-co-repressor complex to PC enhancers in CCs, leading to de-repression of the associated PC genes in CCs. (D) Ubiquitous Notch signaling drives expression of target genes for PC enhancers in all cells of the heart, both as a consequence of the alleviation of repression by the elimination of the Su(H)-co-repressor complex, and due to direct activation by the N^{icd}-Su(H) complex.

Supplementary Table S1. The genomic coordinates of heart, PC and CC enhancers, and orthologous sequences comprising the training sets utilized in this study, along with a list of genes with validated expression in the heart and its subsets (Ahmad et al., 2012). Enhancer orthologs were extracted from the 11 other sequenced *Drosophila* species by searching for regions with at least 50% but less than 80% sequence identity and similar length, GC-content and repeat density as their *D. melanogaster* counterparts (Busser et al., 2012a).

Download Table S1

Supplementary Table S2. Design of the motif-alone and motif+ChIP classifiers, the genomic coordinates and rank of all predicted enhancers from the classifiers, and descriptions of the activities of tested predicted enhancers. To build cell type-specific enhancer prediction models, we generated controls that were randomly sampled from *D. melanogaster* non-coding regions and had similar length, GC- and repeat-content to the training enhancers. Ten control sequences were retrieved for each training enhancer. Each sequence (either enhancer or control) was then scanned using MAST (Bailey and Gribskov, 1998) for 1019 TF binding motifs that were collected from TRANSFAC, JASPAR and uniProbe libraries (Wingender et al., 2001; Sandelin et al., 2004; Berger et al., 2006) and were present among our sequences. To this end, each DNA sequence was converted into a 1019-dimension vector in which a value indicates the counts of TF binding motif per 1000 bp along the considered sequence. We then used a linear support vector machine (SVM) (Cortes and Vapnik, 1995) provided in the libSVM library (Chang and Lin, 2011) to discriminate between enhancers and controls. We used a standard 10-fold cross-validation procedure to assess the discrimination capability of the constructed classifiers. In this procedure, the training set enhancers and corresponding controls were randomly partitioned into 10 disjointed and equal-sized subsets, with each subset being used in turn to test a cell type-specific classifier built with the remaining 9 subsets. In order to evaluate the classification performance reliably, we ran this 10-fold cross-validation procedure 20 times with independent partitioning of samples. See Fig. 2 for the results. In addition, to avoid information leak during cross-validation procedure, an enhancer and its orthologs were always put into the same sample set (either training or test sample set). With the trained classifiers (heart, CC, and PC), we scanned the genome of *D. melanogaster* (BDGP Release 5 assembly) to predict new enhancers. A 500 bps sliding window with a 250 bps incremental step was used for the genome scan. In total, we scored 376,586 sequences. The enhancer cutoff score was set according to the FPR established using a 10-fold cross-validation. Using the setting of FPR=0.01, we detected 2682 heart enhancers, 2962 CC enhancers and 1907 PC enhancers by using motif+ChIP classifiers (Supplementary Fig. S2). Prediction accuracy for each classifier was evaluated by examining the fraction of cardiac enhancers reported in an independent study (Jin et al., 2013) at different FPR cutoffs (Supplementary Fig. S3) and by utilizing genomic site-specific transgenic reporter assays to test 80 enhancer predictions with varying scores in the classifier rankings for the different enhancer models (Fig. 3, Supplementary Fig. S4).

Download Table S2

Supplementary Table S3. DNA sequence motifs and weighting factors identified by the motif-alone and motif+ChIP classifiers.

Download Table S3

Supplementary Table S4. Quantitative summary and statistical significance of the effects of mutating Myb binding sites in the *Ndg* enhancer, the effects of loss-of-function of Myb on the activity of the WT *Ndg* enhancer, and detailed quantitation of the cell division defects associated with the different genotypes examined in this study. Confidence intervals for the mean number of *Ndg* enhancer-expressing CCs per hemisegment were computed using bootstrap methods (Davison and Hinkley, 1997) (see also Fig. 5). Specifically, for a given genotype, the embryos were sampled with replacement to construct a sample of the original size and the mean number of *Ndg* enhancer-expressing CCs per hemisegment was calculated. This process was repeated 10,000 times and an empirical distribution of mean values was obtained. The 95% confidence interval is given by ($\text{mean}_{0.025}$, $\text{mean}_{0.975}$) where $\text{mean}_{0.025}$ designates the 250th smallest of the 10,000 empirical means and $\text{mean}_{0.975}$ designates the 9570th smallest of the means. Permutation testing (Good, 1994) was used to obtain p-values for testing for differences between *Ndg* enhancers (supplementary material Table S4A). Permutation testing (Good, 1994) was also used to obtain p-values for testing the hypothesis that the average number of defects per hemisegment is equivalent in two genotypes (supplementary material Table S4C, Row 1). A bootstrap approach (Davison and Hinkley, 1997) was used to obtain p-values for determining whether non-additive interactions exist among mutation types (supplementary material Table S4C, Rows 2-4). A bootstrap sample was drawn from the genotype with both mutations and the proportion of cell division errors for the genotype was calculated. This average was subtracted from the sum of averages obtained from bootstrap samples of each of the two genotypes with one mutation. From this subtraction a single estimate of the interaction was obtained. The procedure was repeated 10,000 times. P-values for the hypothesis of no interaction were obtained by examination of the proportion of 10,000 bootstrapped interactions above and below 0.

Download Table S4